Boosting the photodynamic activity of erythrosine B by using thermoresponsive and adhesive polymeric systems containing cellulose derivatives for topical delivery

Jéssica Bassi da Silva[a], Rafaela Said dos Santos[a], Camila Felix Vecchi[a], Katieli da Silva Souza Campanholi[b], Ranulfo Combuca da Silva Junior[b], Lidiane Vizioli de Castro Hoshino[c], Wilker Caetano[b], Mauro Luciano Baesso[c], Fernanda Fogagnoli Simas[d], Michael Thomas Cook[e]; Marcos Luciano Bruschi[a,*]

[a]*Laboratory of Research and Development of Drug Delivery Systems, Postgraduate Program in Pharmaceutical Sciences, Department of Pharmacy, State University of Maringa, Maringa, PR, Brazil*

[b]*Department of Chemistry, State University of Maringa, Maringa, Brazil*

[c]*Department of Physics, State University of Maringa, Maringa, Brazil*

[d]*Laboratory of Inflammatory and Neoplastic Cells, Cell Biology Department, Section of Biological Sciences, Federal University of Parana, Curitiba, Brazil*

[e] *UCL School of Pharmacy, University College London, London, WC1N 1AX, UK*

* Corresponding author:

Laboratory of Research and Development of Drug Delivery Systems, Department of Pharmacy, K68 building, room 210, State University of Maringa, 87020-900, Maringa, PR, Brazil.

E-mail address: mlbruschi@uem.br (M. L. Bruschi).

ABSTRACT

Erythrosine displays potential photodynamic activity against different microorganisms and unhealthy cells. However, erythrosine has high hydrophilicity, negatively impacting on permeation through biological membranes. Combining biological macromolecules and thermoresponsive polymers may overcome these erythrosine-related issues as well as enhancing retention of topically applied drugs. Therefore, the aim of this work was to investigate the performance of adhesive and thermoresponsive micellar polymeric systems, containing erythrosine in two states: neutral (ERI) or disodium salt (ERIs). Optimized combinations of poloxamer 407 (polox407) and sodium carboxymethylcellulose (NaCMC) or hydroxypropyl methylcellulose (HPMC) were used as platforms for ERI/ERIs delivery. The rheological and mechanical properties of the systems was explored. Most of the formulations were plastic, thixotropic and viscoelastic at 37 °C, with suitable gelation temperature for in situ gelation. Mechanical parameters were reduced in the presence of the photosensitizer, improving the softness index. Bioadhesion was efficient for all hydrogels, with improved parameters for mucosa in contrast to skin. Formulations composed of 17.5% polox407 and 3% HPMC or 1% NaCMC with 1% (w/w) ERI/ERIs could release the photosensitizer, reaching different layers of the skin/mucosa and ensuring enough production of cytotoxic species for photodynamic therapy. Functional micelles could boost the photodynamic activity of ERI and ERIs, improving their delivery and contact time with the cells.

1. Introduction

Photodynamic therapy consists of administering and irradiating a non-toxic photosensitizer (PS), with a light source of suitable wavelength [1]. Once excited, the PS can transition from excited singlet to triplet state, which possesses a lifetime long enough to allow reactions with neighboring oxygen molecules, producing highly reactive cytotoxic species [2]. The reactive oxygen species or free radicals produced are able to disrupt cytoplasmic membrane [3], increasing the permeability of numerous prokaryotic and eukaryotic cells, as well as causing oxidative damage to intracellular targets [4] and changing metabolic pathways [5]. As the main photodynamic agent, the singlet oxygen can lead unhealthy cells or microorganisms to apoptosis and necrosis [6]. This non-invasive therapy has demonstrated potential in treating primary and advanced carcinomas, also showing promising results in external lesions. The literature reports treatment of squamous cell carcinoma [7], metastases in head or neck regions [8], urological condyloma acuminate [9], skin cancer [10], microbial lesions associated with bone regeneration for peri-implantitis treatment [11], bacterial biofilms [12] and, virus or fungal lesions [13]. In comparison to other treatments, photodynamic therapy can, additionally, offer high selectivity and minimal systemic toxicity. Besides high effectiveness on multiple drug-resistant cells, the therapy may also be a synergistic adjuvant treatment when combined with other therapeutic modalities [14,15].

There are many PS options available, including phenothiazine dyes, phthalocyanines, and porphyrins. Among this class, erythrosine, a xanthene, has garnered significant attention. Its non-toxic behavior added to its existing use in dentistry and food products, makes its translation into the clinic lower risk than for other PS substances [16,17]. Erythrosine is used as a dye used to detect dental biofilms and, has shown potent photodynamic activity reducing the growing of *Streptococcus mutans* [18] and buccal candidiasis [16,17]. Furthermore, Garg and collaborators observed an effective activity of this PS to treat malignant and pre-malignant

oral cell lines, which suggests a possible antitumoral activity in the presence of light [17]. Its potential for treating sinusitis has also been demonstrated, with high efficacy against *Staphylococcus aureus*, when incorporated into a nanoparticulated system [19].

Despite erythrosine's positive photodynamic properties, its hydrophilicity also leads to low permeability through cell membranes [17]. Since the photodynamic activity is related to factors as cellular uptake kinetics of the PS and its subcellular localization profile [20], attempts have been made to alter erythrosine chemistry and solve this issue. For instance, previous studies have investigated the addition of alkyl moieties to its carboxylate group, bring out ester formation, as an alternative to increase the hydrophobicity of the molecule [21,22]. However, alteration of drug chemistry is typically unfavorable due to the need for additional clinical studies, where the novel molecule would be considered a new chemical entity by regulators. Moreover, highly hydrophobic compounds have low water solubility, which may foster PS self-aggregation and reduction of light absorption and single oxygen production [21]. Therefore, the incorporation of this dye in a micellar polymeric system, such as poloxamer-based, besides boosting monomerization of the PS [23,24], is an attractive strategy promote delivery to the cells without altering pharmacological performance.

Poloxamers are a class of triblock copolymer with the general structure of poly(ethylene oxide)$_x$-b-poly(propylene oxide)$_y$-b-poly(ethylene oxide)$_z$ - (PEO$_x$-PPO$_y$-PEO$_z$). Particularly, poloxamer 407 (polox407) is a thermoresponsive copolymer with the structure PEO$_{101}$-PPO$_{65}$-PEO$_{101}$, which is highly attractive in the development of drug delivery systems due to its safety and low-cost [25]. Its local tolerance is satisfactory [26], even when applied as treatment of thermal burns [27]. Solutions of poloxamer exhibit critical micellization temperatures (CMTs), when above the critical micellization concentration (CMC). Therefore, heating poloxamers from below to above CMT, typically results in the formation of ca 10 nanometer spherical micelle with a hydrophobic PPO core and a hydrophilic PEO shell [28], which may carry PS

such as erythrosine. Because of the nanometric size of the micelles, poloxamers have displayed accumulative behavior in tumoral environment due to the increased vascular permeability and low lymphatic drainage, enhancing the efficiency of chemotherapeutics and decreasing chances of side effects [29,30]. Furthermore, when in water dispersions, in appropriately concentration (> ca 15 %, w/v) and above CMT, polox407 exhibits a reversible transition from liquid to a elastic gel mesophase, a result of the spherical core-shell micelles packing into a cubic liquid crystalline structure, as observed by small-angle neutron scattering [31,32]. This property enables a cool solution to flow and become viscous when in contact with the body temperature.

As a hydrogel, polox407 dispersions is believed to mimic biological tissues and have high biocompatibility [33–35], alongside the advantage of the *in situ* gelation triggered by the body's heat, and the smooth texture given by a high degree of well-ordered water. Moreover, the combination of this thermoresponsive polymer with biomacromolecules opens the possibility of combining *in situ* gelation with further functionalities, in order to construct advanced nanocarriers in drug delivery field [36]. Therefore, polymer blends containing polox407 and other additives have been extensively studied as an advantageous strategy for the development of topical drug delivery platforms. For instance, polox407 systems may be able to improve the retention at a topical site with the use of mucoadhesive polymers, such as polycarbophil [37], Carbopol 971P® [38], Carbopol 974P® [39], Carbopol 934P® [30,33,34,40,41] or cellulose derivatives [42–45].

Particularly, for topical drug delivery, systems containing polox407 and hydroxypropyl methylcellulose (HPMC) or sodium carboxymethylcellulose (NaCMC) as mucoadhesive biological macromolecules are promising with respect to their rheological, mechanical, micellar and adhesive characteristics [42–47]. Both cellulose derivatives present good adhesiveness combined with the ability to form strong hydrogels [48]. As a result, the additives not only contribute to the optimization of polox407 hydrogel strength, but also improve its

adhesion to mucosa or skin [42]. Therefore, this study aims to investigate the performance of the adhesive and thermoresponsive micellar systems, composed of polox407, HPMC or NaCMC and, erythrosine; which was used in its neutral form (ERI) or its disodium salt (ERIs). Furthermore, the photodynamic activity of those micellar systems was tested on non-tumoral fibroblasts and melanoma tumor cells in comparison with pure erythrosine (ERI and ERIs), allowing for a complete comprehension of the effect of the polymeric systems on the erythrosine photodynamic activity.

2. Materials and methods

2.1. Materials

Poloxamer 407 (polox407), erythrosine B [ERI; neutral form; saturation solubility 0.7 mg/mL [49]] and its disodium salt [ERIs; saturation solubility 70 mg/mL [50]], mucin (from porcine stomach, type II crude), uric acid, and phosphate buffered tablets (pH 7.4) were purchased from Sigma-Aldrich (Sao Paulo, SP, Brazil). HPMC K100, Methocel® (8.1% hydroxypropoxyl 22% methoxyl content) was kindly donated from Colorcon Dow Chemical Company™ (Dartford, United Kingdom). NaCMC (DS = 0.8-0.95) was purchased from Synth (Diadema, SP, Brazil). Ultra-purified water was obtained in-house using a Milli-Q water purification system (Darmstadt, Germany). All reagents were used without further purification.

2.2. Preparation of thermogelling formulations

Thermogelling systems were prepared by dispersion of 3% (w/w) HPMC or 1% (w/w) NaCMC in purified water, under magnetic stirring at room temperature. After the cellulose derivatives were completely dispersed, 17.5% (w/w) polox407 was added to the preparations and the mixtures were stored at 5 °C for 48 h, allowing swelling and partial dissolution of polymer. After this wait, the polymeric systems were stirred again to complete the dissolution

6

of the remaining polymers. Two states of erythrosine B were explored. Native ERI at 95% purity (ERI) and its disodium salt (ERIs) were added to the formulation at a level of 1% (w/w), with magnetic stirring, prior to the addition of polymers [17]. Formulations were kept at 5 °C for at least 24 h prior to analysis [37,51,52].

2.3. Rheology

Rheological measurements were performed with a controlled stress rheometer (MARS II, Haake Thermo Fisher Scientific Inc., Germany) using a parallel steel cone-plate geometry (35 mm, gap of 0.105 mm). All the analysis was performed at three temperatures: 5, 25 and 37 °C. The samples were carefully placed to the inferior plate and allowed to attain their equilibrium state for at least one minute before starting analysis. At least three replicates of each sample were analyzed.

2.3.1. Continuous shear analysis

In flow mode, the up curve was measured over 150 s, with shear rates ranging from 0 to 2000 s^{-1}. The system was kept at the maximum shear rate for 10 s and, then, decreased over 150 s from 2000 to 0 s^{-1}, obtaining the down curve [39,52,53]. The up curve was fitted by Oswald-de-Waele equation Eq. (1):

$$\sigma = k\dot{\gamma}^n \tag{1}$$

where σ is the shear stress (Pa), K is the consistency index $(Pa.s)^n$, $\dot{\gamma}$ is the rate of shear (s^{-1}), and n is the flow behavior index (dimensionless). Yield stress values were investigated by the Casson equation Eq. (2) [54]:

$$\sigma = \sqrt[n]{\left(\sigma_y^n + (\dot{\gamma} n_p)\right)^n} \tag{2}$$

where σ represents the shear stress (Pa), n is the flow behavior index (dimensionless), σ_y is yield stress (Pa), $\dot{\gamma}$ is the shear rate (s^{-1}) and n_p is Casson plastic viscosity. Hysteresis area of each system was calculated using RheoWin 4.10.0000 (Haakes®) software.

2.3.2. Oscillatory measurements

The viscoelastic properties were assessed in oscillatory mode. Firstly, for each system, the linear viscoelastic region (LVR) was determined. Frequency sweep analysis was then conducted from 0.1 to 10.0 Hz [39,52,53]. The storage modulus (G'), loss modulus (G"), dynamic viscosity (η') and loss tangent (tan δ) were obtained by RheoWin 4.10.0000 (Haakes®) software.

2.3.3. Determination of sol-gel transition temperature ($T_{sol/gel}$)

The determination of $T_{sol/gel}$ was performed in oscillatory mode. A temperature ramp ranging from 5 to 60 ºC at 1.0 Hz of frequency was performed. The assay was conducted using a controlled stress within the LVR, under a heating rate of 10 °C/min. G', G", η' and tan δ were calculated using the same software above described. The temperature at which the elastic modulus (G') was halfway between the values for the solution and gel was defined as $T_{sol/gel}$, based on a significant increase of dynamic viscosity (η') as the temperature increased [39–41,52,53].

2.4. Texture profile analysis (TPA)

The evaluation of mechanical textural characteristics of the formulations was conducted using a TA-XTplus texture analyzer (Stable Micro Systems, Surrey, UK), in TPA mode, at 5,

8

25 and 37 °C. Glass bottles were filled with ca 16 g of the samples, avoiding air bubbles. The systems were compressed twice by a 10 mm diameter analytical probe. The compressions were performed at 2 mm/s, to a depth of 15 mm. Between the end of the first compression and the beginning of the second one, there was a delay time of 15 s. Hardness (the largest force on first compression), compressibility (work required to deform the formulation in the first compression), adhesiveness (work required to overcome the attractive forces between probe and sample), elasticity (the ability to stretch and return to its original state), and cohesiveness (the restructuring ability, after a double compression be applied) were calculated from the force-time and force-distance graphs as detailed elsewhere [39–41,44,52,53].

2.5. Determination of softness index

The softness index of each formulation was assessed by texture analyzer, in compression mode, at 37 °C, using a Perspex conic probe (P/45C). 50 mL beakers were filled with the preparations. The analytical probe was compressed into each formulation at 1 mm/s, and to a depth of 10 mm. The softness index was considered the maximum force obtained as the probe penetrates in each sample - calculated as the maximum value in a force-distance graph, as detailly reported elsewhere [39,40,44,53].

2.6. Bio/mucoadhesion assessment

The bioadhesive properties of the hydrogels were assessed using the TA-XTplus texture analyzer (Stable Micro Systems), with mucin disk or animal skin tissue as substrate. The skin tissues used were porcine ear skin obtained from a local slaughterhouse. These tissues were immediately collected after the slaughter of the animals, washed with purified water, and prepared. The excision was made from the dorsal ear skin using a scalpel, before being kept on the freezer [30]. Several hours before testing, the tissues were defrosted at room temperature

and placed into a support (polypropylene sample vial). Thus, only a 4 mm diameter circle of the skin came into contact with the thermogelling formulations [52].

The substrates were attached to mobile cylindrical probe (10 mm of diameter) using a double-side adhesive tape. The probe was lowered at a speed of 1 mm/s until it reached the surface of each hydrogel evaluated, which were kept partially immersed in purified water at 37 $\pm$ 1 ºC for 30 min prior the analysis. Contact force was 0.03 N, which kept the substrate just in contact with the hydrogel surface. Substrate and formulation remained in contact for 30 s, with the probe withdrawing at a rate of 10.0 mm/s until the complete detachment of the adhesive hydrogels from the mucin disks or animal tissue. The maximum force of detachment and the work of adhesion, calculated area under the force/distance curve, were determined by using Texture Exponent 3.2 software (Stable Micro Systems). All the measurements were performed at least three times for each sample and presented as mean values $\pm$ standard deviation.

2.7. Determination of tissue permeation by photoacoustic spectroscopy

Skin samples were taken from the ear of young, freshly slaughtered, white pigs from a local slaughterhouse. The porcine buccal mucosa was obtained from the same animals. After cleaning, the subcutaneous fat was carefully removed from the skin, while the mucosa was excised from the cheek. Both samples were cut in a square shape using scissors and a surgical scalpel, with skin taken from the central region of the dorsal side of the ear. Samples with wounds, warts, or hematomas were not used. The porcine tissues were stored at −18 °C until the day of the experiment, when they were unfrozen at room temperature [34].

The permeation of ERI and ERIs from the polymeric systems was performed in ear porcine skin and porcine buccal mucosa by photoacoustic spectroscopy (Fig. S5). Ca 30 µg of each formulation was homogeneously placed on the surface of 1 cm^3 tissue. After 30 min, the samples were evaluated by the equipment as described in SI. The final photoacoustic signal is

proportional to the sample absorption coefficient. Hence, the photoacoustic spectra can be interpreted by means of bands absorption [55,56]. All spectra were normalized with respect to a carbon black sample signal, correcting the source emission intensity in each wavelength. The spectra of each ear and mucosa were obtained between 300 and 650 nm, positioning the sample into the photoacoustic cell and illuminating the face to be measured (Fig. S6). Afterwards, the tissues were turned to illuminate the opposite side. Detecting the presence of ERI or ERIs band on the dorsal side (opposite side of application) indicates the locally applied formulation permeated through the ear or buccal tissue [57]. The detection of ERI and ERIs on different layers of the tissues may reflect either the permeation of the micellar systems in combination with drug release or, in fact, the permeation of the free drug.

2.8. Evaluation of photodynamic activity

The evaluation of photodynamic chemical activity of the formulations was determined using a method [4,58,59] adapted from Fischer et al. [60]. Ca 28 mg of each formulation, at 5 °C, was deposited at the bottom of a quartz cuvette with a 1.0 cm optical pathlength (Fig. S7). They were allowed to warm over two minutes. Uric acid (UA), an extensively explored chemical probe, was used to evaluate singlet oxygen and generation of other reactive oxygen species. The UA solution was prepared in 2 M NaOH medium and diluted in carbonate-bicarbonate buffer (pH 7.4) attaining a concentration of 0.5 µmol/L [61]. The diluted UA solution was carefully added to the ERI- or ERIs-systems already placed in the cuvette, which was inserted in a holder, positioned on a UV-Vis spectrophotometer (Cary 50 model). On the equipment, six LEDs with average fluency $\pm$ standard deviation of $3.14\text{x}10^4 \pm 2.44\text{x}10^3$ µWatt/cm^2 and λmax = 593 nm were coupled, as demonstrated in Fig.S9. External light had no influence on the measurements due to the modulated phase radiation used. The reduction of

the 293 nm band, relative to UA degradation, was monitored at room temperature [58,62], and the degradation kinetics were interrupted after reaching infinity.

2.9. Phototoxicity assay

HPMC/polox407 and NaCMC/polox407 systems with and without ERI or ERIs were lyophilized and diluted in sterile DMEM culture medium (at 50 µg/mL), meanwhile ERI and ERIs solutions were also prepared in sterile DMEM at 0.5 µg/mL, which correspond to the amount of erythrosine present in respective binary polymeric systems (1% of the total compounds).

Phototoxicity assay was carried out with melanoma B16-F10 murine melanoma (BCRJ, 0046) and non-tumorigenic fibroblasts BALB/3T3 clone A31 (ATCC, CCL-163) cell lines. Cells were cultured in DMEM containing 1.5 mg/L sodium bicarbonate, 1 U/mL penicillin, 1 µg/mL streptomycin, and 10% FBS. Cells were maintained at 37ºC in humidified atmosphere with 5% CO_2. For seeding, cells were washed with PBS, detached using trypsin/EDTA, counted in hemocytometer and seeded in 96-well plates (7,000 and 2,500 cells/well to fibroblasts and melanoma cells, respectively). The cells were incubated over 24 h and then exposed to polymeric systems with or without ERI or ERIs (at final concentration of 0.1 µg/mL) Pure ERI and ERIs were tested at final concentration of 0.1 µg/mL. Plates were incubated at 37 °C in an atmosphere with 5% CO_2 for 3 h and then they were exposed to the suitable light wavelength (525 nm) for 15 min (energy dose = 12 J/cm^2). After the light exposure (18 h), the phototoxicity of the systems and ERI (or ERIs) was assessed by MTT (Thyazolyl Blue Tetrazolium Bromide) assay. The cells were incubated with 0.5 mg/mL MTT solution for 3 h, the resulting formazan crystals were eluted using DMSO (100 µL), and absorbance was measured at 550 nm [63]. The cytotoxicity of the systems and the pure ERI/ERIs was evaluated in comparison to the non-treated cells. The phototoxicity, in turn, was

evaluated by the comparison between the results obtained in cells treated but not exposed to light.

2.10. Statistical analysis

The effects of cellulose derivative type, active content, and temperature on textural (hardness, compressibility, adhesiveness, elasticity and cohesiveness) and rheological properties (consistency index, flow index, yield stress and hysteresis area) were statistically compared using three-way analysis of variance (ANOVA). Similarly, the effects of bioadhesive polymer concentration and type on softness index were statistically evaluated using two-way ANOVA. In all cases, individual differences between means were identified using Tukey's honestly significant difference test. The paired Student's *t*-test was used to determine if the dynamic viscosity (η') of the formulations increased with rising temperature ($T_{sol/gel}$). Detachment force and work adhesion for both substrates were treated with two-way ANOVA (multiple comparisons), using Tukey's *post-hoc* test. Significant differences were accepted when $p < 0.05$ and Statistica 8.0 software (StatSoft Company) was used throughout. All cytotoxicity phototoxicity experiments were performed in four biological independent experiments with technical quadruplicates and the data were presented as the medians, which were compared using Mann-Whitney non-parametric test (* represents significative differences with $p<0.05$).

3. Results and discussion

3.1. Rheological characterization

Rheological analysis was initially conducted on the conmposite gel systems. Rotational shear rheology submits the sample to a large strain, so that the samples deform and have lost their internal structure at rest [64]. The consistency index (*K*) gives information regarding the

viscosity at low shear, and is reflective of the "hanging point" of the rheogram as the shear rate approaches zero. For thermogelling systems, high values of K are expected at high temperatures, at which the systems are in the gel mesophase (Fig. 1). As the gelation proceeds, the systems present great resistance to flow due to the entanglement of polymeric chains and presence of a concentrated micellar system. NaCMC systems demonstrated significant reduction in K values when in the presence of drug, attributed to the repulsion between ionic species of NaCMC and ERI/ERIs or salting out effects [23]. For HPMC preparations, there was not a significative ($p<0.05$) difference between the ERI or ERIs systems and those without the PS.

Polox407 formulations with NaCMC and HPMC were prepared for evaluation as a drug delivery platform, which show potential for application to mucosal surfaces, such as the oral or vaginal mucosa [44]. Both NaCMC and HPMC systems, with or without ERI and ERIs, demonstrated shear thinning behavior (Fig. 1). This is attributed to chain rearrangement. With increasing stress, their polymeric chains became aligned according to shear direction, with a reduction of the apparent viscosity of the system observed [41,44]. The increase in temperature predominantly reduced the flow behavior index (n) in all polymeric systems evaluated. Preparations containing ERI or ERIs demonstrated a similar reduction in n; however, this effect was small when compared with formulations without drug. As n index reflects the structure of the semi-solid formulation in terms of free water available, a low amount of free water leads to non-Newtonian behavior, reducing this index further from one unit [41]. Systems with drug displayed high n values, if compared to the formulation without the PS, suggesting some disruption of structure in both formulations.

NaCMC systems demonstrated plastic behavior (with yield stress) at 5ºC, while the HPMC ones displayed a pseudoplastic profile (without yield stress), as shown on Fig. 1 and Fig. S1. There was an increase in yield value when the temperature increased for both

14

preparations. As thermoresponsive hydrogels, their viscosity also increased in a similar way to that observed for K values. High yield values support topical application of semi-solid systems, suggesting increased *in vivo* retention due to an increased resistance to flow [38]. Comparing the effect of ERI or ERIs into NaCMC systems, ERIs demonstrated yield values lower than ERI, comparable to the formulation without the PS. The density of charges may promote repulsive effect, mainly for the disodium salt, which is predominantly in its dianionic form, as reported elsewhere [23]. In this case, less stress may be necessary to the samples start flowing. In preparations composed of HPMC, the yield values observed were quite similar among formulations with or without ERI or ERIs. However, ERIs increased the plasticity of the systems at 37 °C, while ERI decreased it. Overall, HPMC presented a low impact on polox407 structure, whilst the PS have been reported to interact in an improved manner with polox407 [23]. Then, ERI and ERIs may be better accommodated into this micellar system, slight impacting rheological parameters.

Polymeric dispersions may undergo reversible loss of viscosity when submitted to shear stress, which is revealed by the hysteresis area obtained from subtraction of the downcurve from the area of the upcurve during rotational shear rheology. A thixotropic behavior is given by a positive hysteresis area, meanwhile a negative one denotes rheopectic profile [39,41]. At 5 °C, most systems presented thixotropic behavior, with rheopectic profile only observed for systems with ERIs. NaCMC systems were all thixotropic at 25 °C, while HPMC ones showed a rheopectic profile at this temperature. Nonetheless, at 37 °C all of them demonstrated thixotropic behavior, favoring their use as local drug delivery systems [39]. During the application, the stress makes the system less viscous, assisting its ability to be spread. Thus, when the stress ceases, the samples can recover its initial structure, though with reduced viscosity, in a small period of time if compared to rheopectic systems.
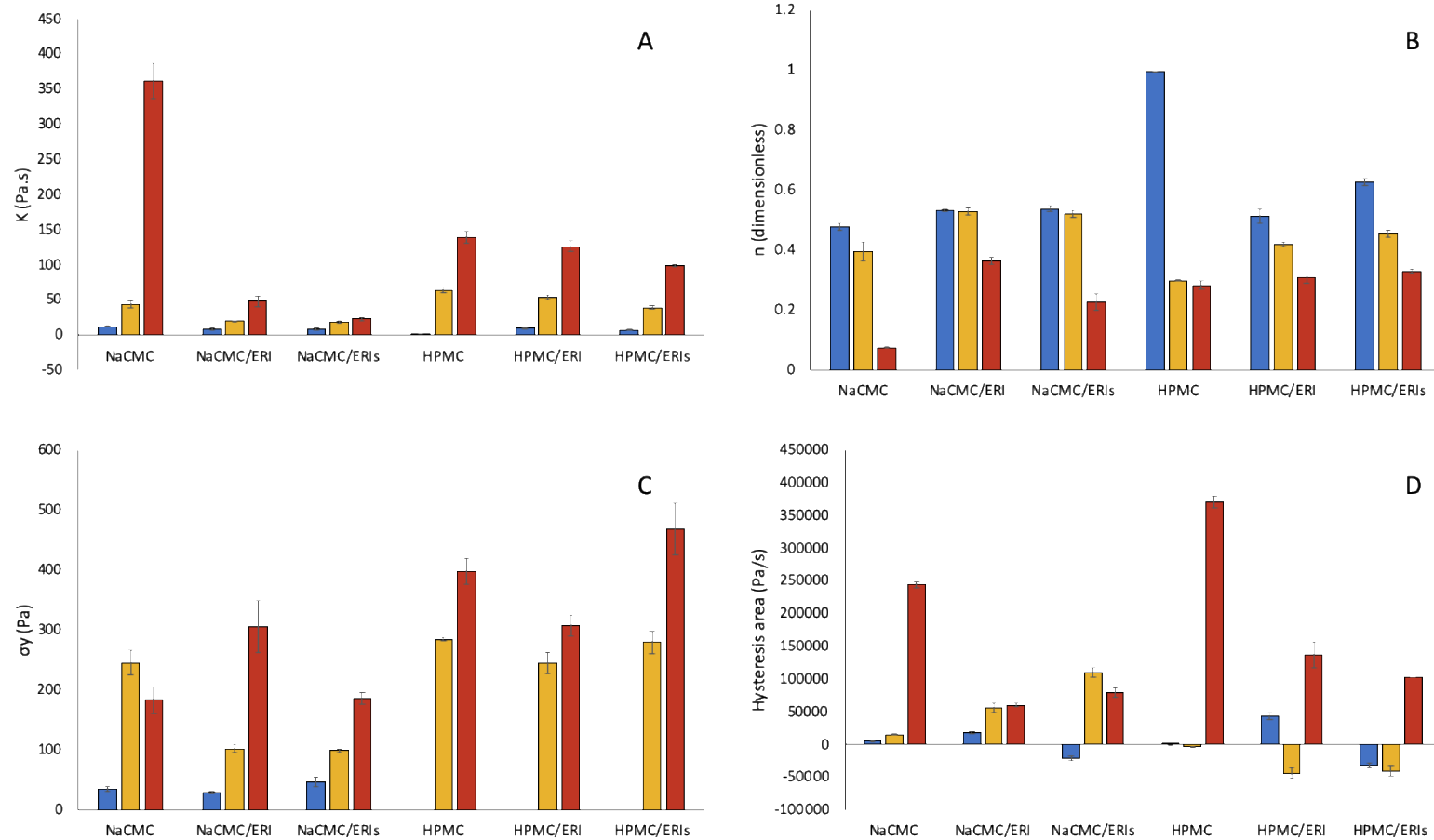
Fig. 1. The effects of presence of neutral erythrosine (ERI) or disodium erythrosine (ERIs) in binary polymeric systems composed of poloxamer 407 (polox407) and hydroxypropyl methylcellulose (HPMC) or sodium carboxymethylcellulose (NaCMC) on the consistency index (K, A), flow behavior index (n, B), yield value (σ_y, C) and hysteresis area (D) at 5 (blue), 25 (yellow) and 37 ℃ (red).

Oscillatory rheometry evaluates the viscoelastic properties of semi-solid preparations at low shear, simulating their behavior in conditions similar to a physiological environment under rest [44]. Elastic (G') and viscous (G'') moduli are related to the stored and dissipated energy, respectively, in each deformation cycle at a specific frequency [41,65]. The ratio of G'' by G' allows for the calculation of tan δ (G''/G'), which may have values higher or lower than one (but not less than 0), characterizing elastoviscous or viscoelastic formulations, respectively [37].

The cellulose type, oscillatory frequency, temperature, and the presence of PS affected the viscoelastic properties of the formulations. Overall, few changes in viscoelastic properties were observed with PS presence and all systems exhibited viscoelastic behavior at 37 °C. All NaCMC dispersions were viscoelastic materials at the three temperatures (Table S1 - S4). Increasing oscillatory frequency and temperature lead to a reduction of tan δ values, since there was increase in G' and reduction of G''. As expected, ERIs demonstrated greatest impact on the viscoelastic properties of NaCMC systems. ERIs/NaCMC system presented low elasticity in comparison to ERI and the system without drug, reaching high values of tan δ. Moreover, G' modulus of NaCMC preparations, at 25 and 37 °C, was dominant in comparison to ERIs-NaCMC system, while in comparison to ERI system it was smaller at 37 °C (Fig. 2). High values of G' may be related to high points of connection between the components of the system. Therefore, in agreement with other parameters, ERIs seems to disturb the system, reducing connection points and presenting reduced G'.

In turn, HPMC systems with ERI or ERIs were predominantly viscous at 5 °C (Fig. S2). The preparation without PS displayed the same behavior, with tan δ values higher than one unit at low oscillatory frequencies (Fig. 2, Fig. S3). At 25 and 37 °C, all HPMC polymeric systems were viscoelastic, with this property varying according to the frequency or addition of drug. G' values increased with the oscillatory frequency and temperature, suggesting temporary

networks formation between polymers (Fig. 2). Moreover, it was also observed that ERI and

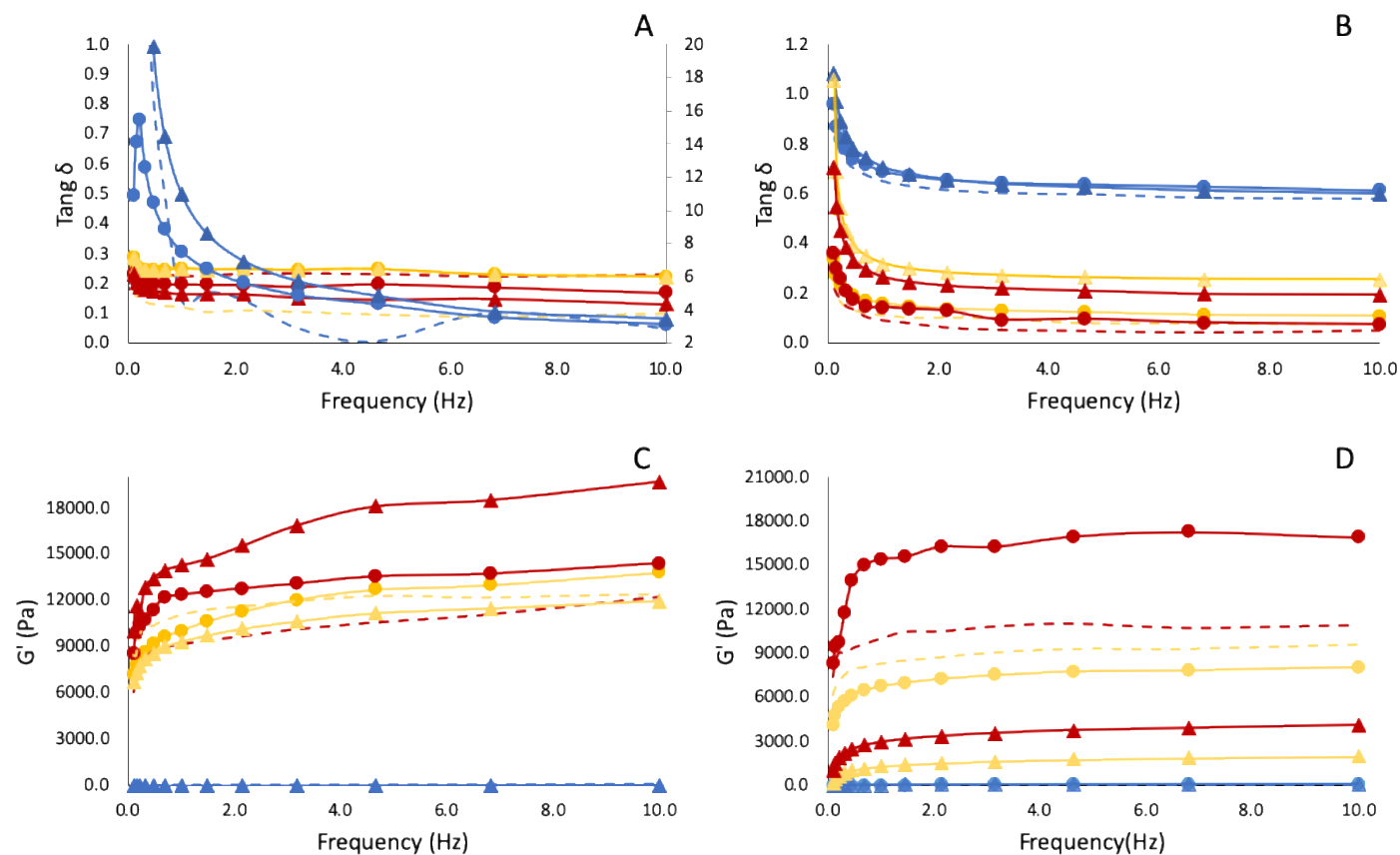ERIs had similar impact on HPMC system, as reported by TEM microscopy before [23].

Fig 2. Loss tangent (tan δ) (A and B) and storage modulus (G') (C and D) as a function of frequency, at temperatures of 5 (blue), 25 (yellow) and 37 °C (red) for 17.5% (w/w) poloxamer 407 and 3% (w/w) hydroxypropyl methylcellulose (A and C) or sodium carboxymethylcellulose (B and D) without (--) or with ERI (●) or ERIs (▲). Each point of the rheogram represents the mean of at least three replicates. Standard deviations have been omitted for clarity; however, in all cases, the relative standard deviation was lower than 12% as exposed in SI.

3.2. Sol-gel transition temperature ($T_{sol/gel}$)

Gelation temperature is the temperature at which a polymeric dispersion changes its behavior from solution to gel. For topical dosage forms, the literature reports a suitable $T_{sol/gel}$ between 25 and 37 °C, which is sufficient to allow for *in situ* gel formation when it is warmed from storage to body temperature [66]. If $T_{sol/gel}$ is higher than 37 °C, the gels will not achieve their elastic properties, resulting in a leakage of the preparations from the application site [67]. Table 1 shows the $T_{sol/gel}$ of all preparations evaluated, with all the formulations demonstrating gelation when warmed to physiological temperature. For systems containing NaCMC, both PS increased the $T_{sol/gel}$, however in the HPMC hydrogel they this value decreased. Additionally, the low $T_{sol/gel}$ observed for HPMC systems may be related to its high viscosity at 37 °C, demonstrated by consistency index, for example. The increased viscosity may facilitate the gelation process since less water would be available.

Table 1

Sol-gel transition temperature ($T_{sol/gel}$) of binary polymeric systems containing poloxamer 407 (polox407) and sodium carboxymethylcellulose (NaCMC) or hydroxypropyl methylcellulose (HPMC), with or without neutral erythrosine (ERI) or disodium erythrosine (ERIs)[a].

Cellulose derivative (%, w/w)		Polox407 (%, w/w)	Photosensitizer		$T_{sol/gel}$ (°C)
			ERI	ERIs	
NaCMC	1.0	17.5	-	-	31.44 ± 0.79
NaCMC	1.0	17.5	1.0	-	32.84 ± 0.54
NaCMC	1.0	17.5	-	1.0	34.68 ± 0.05
HPMC	3.0	17.5	-	-	29.96 ± 0.26
HPMC	3.0	17.5	1.0	-	26.74 ± 0.70
HPMC	3.0	17.5	-	1.0	27.47 ± 0.26

[a] Each mean represents the mean (± standard deviation) of at least three replicates.

Previous studies have demonstrated the effect of numerous additives on the micellization or gelation properties of polox407 [45,68,69]. The critical volume fractions for gelation may be attained at low temperatures with the addition of the drug, since polymer chains experience less water solvation with greater solute quantity [70]. Therefore, the reduced $T_{sol/gel}$ may be explained by considering the higher amount of total solute in HPMC systems (3%, w/w) than NaCMC (1%, w/w) ones, The literature reports hydrophobicity of the solutes and the presence of cosolvents can also have important bearing with such changes [71,72]. Both drugs decreased $T_{sol/gel}$ when into HPMC systems; however, ERI reduced this value to a greater extent than ERIs. As a drug with high hydrophobicity in comparison to ERIs, ERI may provide reduction in the polox407 solvation, leading to low $T_{sol/gel}$ values, agreeing with previous studies [23].

Ionic species, such as NaCMC and ERIs, often salt-out polox407, reducing its micellization and gelation temperature/ However, the reduction of $T_{sol/gel}$ was observed only for non-ionic HPMC preparations suggesting that charged species are not having the expected impact [44,73]. This suggests that interaction and partition of NaCMC and ERIs into PPO and PEO segments, rather than competing for water, attract solvation to polox407. Moreover, as anionic species at physiological pH, ERIs may disturb micellar packing of polox407 when incorporated into the NaCMC system, resulting in its elevation of $T_{sol/gel}$ [74]. Both NaCMC and ERIs, in their anionic form, may repel each other creating space between them. A higher amount of water could, therefore, be entrapped between them, requiring raised temperatures and micellar volume fraction to be achieved prior the system undergoes gelation [23,44,64].

3.3. Mechanical characterization

There are numerous desirable attributes for polymeric semi-solid systems considering pharmaceutical applications. During their development some desirable mechanical properties

may be defined, such as ease of extruding the product out of the package container and spread-ability of the preparation on the skin or mucosal surface. Moreover, suitable adhesion can contribute to the ultimate clinical efficacy of the polymeric system [44,64]. Therefore, the knowledge of comparative mechanical profile of the formulations with or without the active of interest is relevant, since there is intention for topical application [41].

Mechanical properties were dependent on temperature and type of drug [75]. Fig. 3 displays the hardness, compressibility, adhesiveness, elasticity and cohesiveness of the systems evaluated with both cellulose derivatives with or without ERI or ERIs. As already observed when studying the platforms without PS, typically the hardness, compressibility and adhesiveness increased with the increase of temperature. Meanwhile, cohesiveness and elasticity do not demonstrate large differences. This trend is observed for all the semi-solid systems evaluated. Additionally, the presence of ERI or ERIs decreased hardness and compressibility, showing some degree of disruption of the polymeric matrices. ERIs displayed a greater negative impact on hardness and compressibility than ERI. PS solubilization into the micelles, or even to the extra-micellar environment, may increase the distance between the micelles, fostering fewer micellar-micellar interactions and reduced gel strength [73]. Both PSs reduced adhesiveness, with ERIs having a large impact on NaCMC preparations, which may also be related to the ionized state of both additives, carrying out repulsive or steric effect between the polymer and the drug [64].
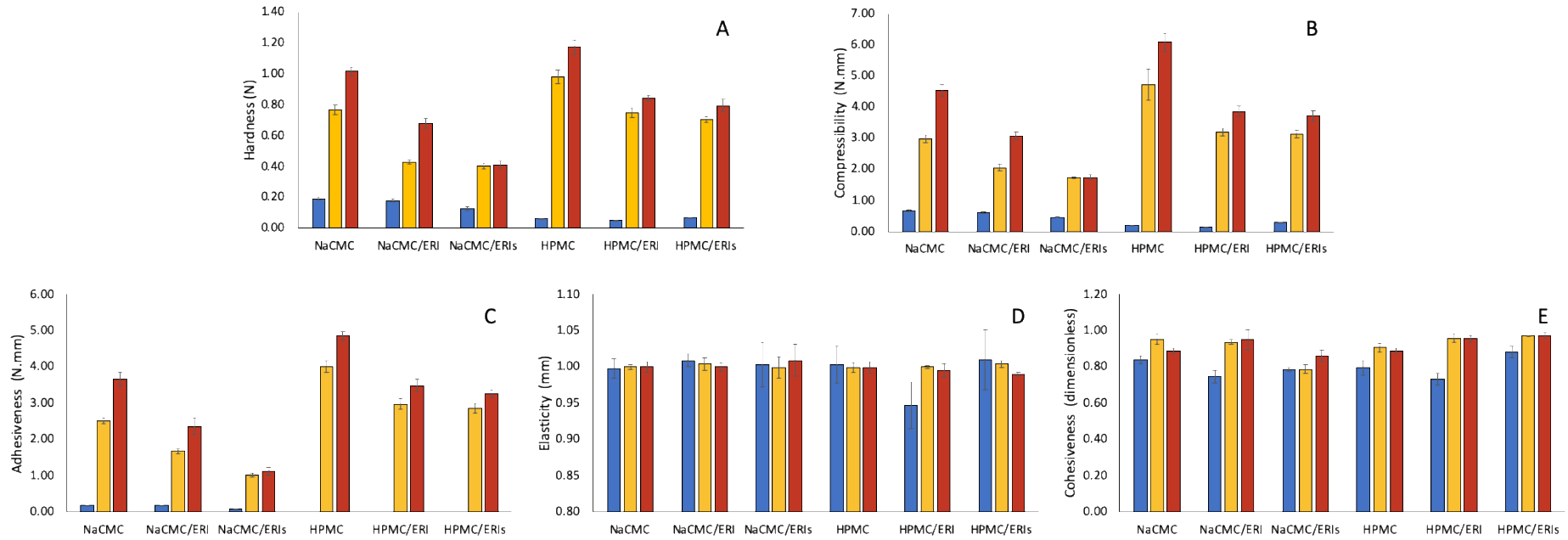
Fig. 3. Texture profile analysis (TPA) parameters of binary polymeric hydrogels composed of 17.5% (w/w) poloxamer 407 (polox407) and hydroxypropyl methylcellulose (HPMC) or sodium carboxymethylcellulose (NaCMC), without[a] or added of neutral erythrosine (ERI) or disodium salt erythrosine (ERIs), at 5 (blue), 25 (yellow) and 37 °C (red). [a][44].

The determination of softness index compliments TPA properties, predicting spread-ability and sensorial evaluation of semi-solid formulations. The technique is able to determine the plasticity of the systems using a specific conical probe [44]. In pursuit of the evaluation of smoothness of the semi-solid formulations, this measurement was performed under physiological conditions in preparations with or without drug. Softness index is determined as the necessary force during penetration of the conic al probe at a depth of 10 mm of the material [39,53], with results displayed in Fig. 4. A higher softness index means systems with higher resistance to the probe (rigidity). Formulations without drug, for both cellulose derivative systems, demonstrated higher rigidity. The presence of ERI or ERIs reduced the softness index of the systems, in agreement with values of hardness by TPA and, k index by flow rheology. Generally, HPMC formulations demonstrated higher softness indexes than NaCMC ones, linked to the higher amount of total solute in them. Among NaCMC systems, ERIs showed the greatest impact on this measurement. It caused reduction in the softness index in comparison with the preparation without drug and the ERI-NaCMC system. For HPMC formulations, the ERI and ERIs had an equivalent negative effect on softness index.
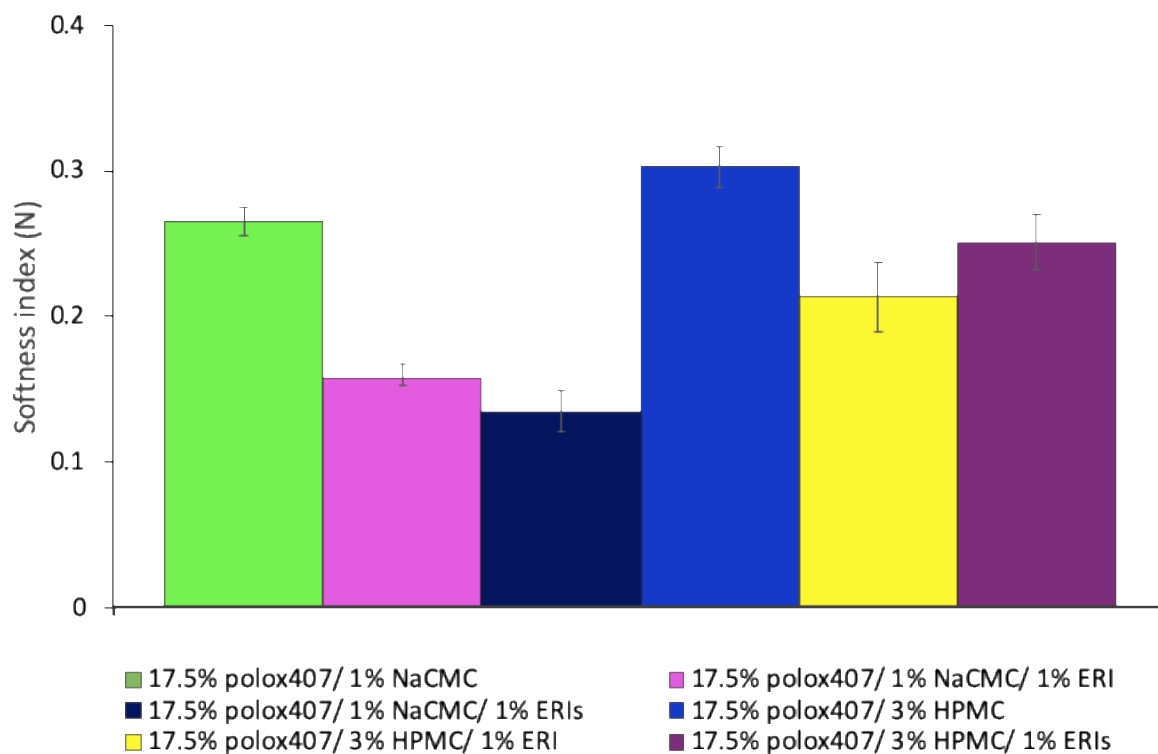
Fig. 4. Softness of binary polymeric systems composed of 17.5% (w/w) poloxamer 407 (polox407) and 1% (w/w) sodium carboxymethylcellulose (NaCMC) or 3% (w/w) hydroxypropyl methylcellulose (HPMC), without or with neutral erythrosine (ERI) or disodium salt erythrosine (ERIs), at 37 °C. Each value represents the mean (± standard deviation) of at least three replicates.

3.4. Bio/mucoadhesion assessment

The tensile strength method is widely used to evaluate the mucoadhesive performance of different formulations, such as solids, liquids and semi-solids. Typically, detachment force and work of adhesion are determined against several types of substrate [76]. Numerous types of animal mucosa [77], synthetic mucosa [52,78], mucin disks [38] or animal skin [79] may be used as substrates, allowing for performance testing of materials and mechanistic study of adhesiveness of the formulations. Fig. 5 displays the results of detachment force and work of adhesion for all polymeric systems containing polox407 and HPMC or NaCMC, using mucin

disk and porcine skin as substrates. It also shows their performance in the presence of ERI or ERIs on substrates. Detachment force represents the measurements of the maximum force necessary to detach the hydrogels from the substrates, while the work of adhesion provides a wider evaluation of the sum of established bonds, including cohesion in the formulation [52,80].
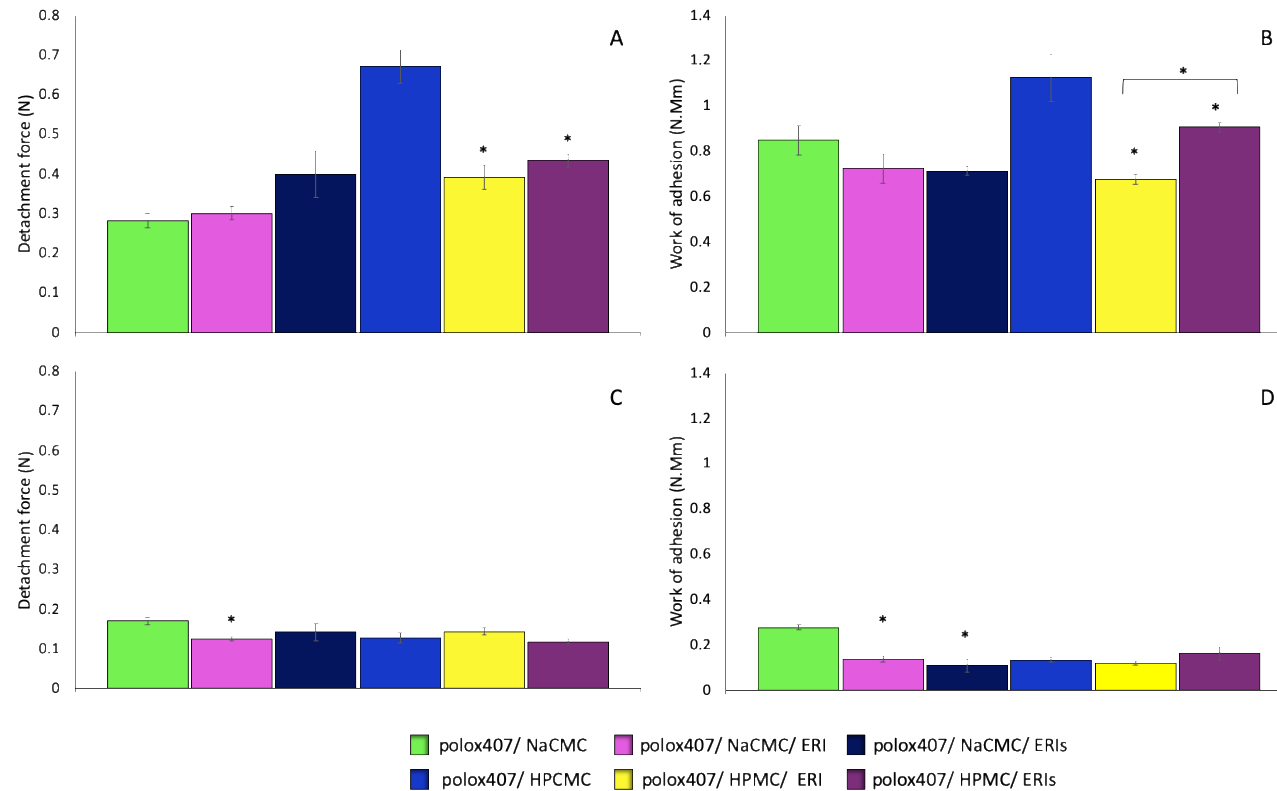
Fig. 5. Determination of mucoadhesion (A and B) and bioadhesion (C and D) by the detachment force (A and C) and work of adhesion (B and D) of binary polymeric formulations containing 17.5% (w/w) poloxamer 407 (polox407) and 3% (w/w) hydroxypropyl methylcellulose (HPMC) or 1% (w/w) sodium carboxymethylcellulose (NaCMC) without or added of 1% (w/w) neutral erythrosine (ERI) or 1% (w/w) disodium salt erythrosine (ERIs) at 37 °C, using a mucin tablet or porcine ear skin as substrates. Each value represents the mean (± standard deviation) of at least three replicates. * Results statistically significative ($p < 0.05$).

Generally, a higher mucoadhesive (to mucin) than bioadhesive (to skin) signal was determined for all the formulations. Evaluating the mucoadhesion using mucin disk by the detachment force or work of adhesion gave no difference among most NaCMC-systems. Significant difference was observed by detachment force between the system without drug and with ERIs, where the ERIs preparation presented higher adhesiveness. For HPMC formulations statistical difference was observed among all systems by work of adhesion ($p < 0.05$). Meanwhile, considering the detachment force, formulations without drug showed the greatest mucoadhesion ($p < 0.05$), whilst HPMC-systems with drug were equivalent. The bioadhesion using porcine ear skin did not show significant difference between most NaCMC and HPMC formulations when measuring the detachment force. The only exception was NaCMC-ERI and its preparation without drug, where there was a significative ($p < 0.05$) decrease in the adhesion performance of the system when adding ERI. By work of adhesion, in turn, there was difference for both ERI and ERIs NaCMC-formulations compared to their control, with no difference between HPMC preparations. Therefore, the bioadhesion for HPMC preparations with or without drug was statistically equivalent by both detachment force and work of adhesion.

Although the formulations were able to establish stronger interactions with mucin than with the skin, they presented good mucoadhesive and bioadhesive ability overall if compared to mixtures containing polox407 and polyacrylic acid derivatives or pure polyacrylic acid derivative solutions [38,39,81]. HPMC preparation, without drug, showed the highest mucoadhesion. Whilst, for bioadhesion, NaCMC systems without drug reached the highest values. The anionic state of NaCMC may impair its mucoadhesive performance in comparison to HPMC formulations due to a repulsive electrostatic effect with mucin, which presents negative net charge under physiological conditions [76,80]. Furthermore, the lower interaction of HPMC and polox407 have been reported in the literature in comparison to NaCMC [44,45], suggesting more HPMC chains are available to perform physical interlocking with mucin

28

chains, improving its mucoadhesive performance. Comparing ERI and ERIs formulations, both had similar adhesive profile; however, ERIs had slightly higher values in the majority of the cases. The addition of ERI or ERIs in NaCMC systems increases its mucoadhesion as measured by detachment force, while they appear to decrease it when incorporated into HPMC preparations. On the other hand, for bioadhesion measurements, by the same parameter, the addition of both drugs leads to a reduction of this property in NaCMC preparations with some inclination to increase it in HPMC systems.

3.5. Permeation study

The *ex vivo* determination of percutaneous permeation was performed by photoacoustic spectroscopy using porcine oral mucosa and skin, which possesses a high similarity to human skin [82,83]. Due to the high reactivity and short half-life of singlet oxygen, only neighboring molecules are affected by PDT, therefore, the localization of the PS is important to the outcome of this therapy [84]. Permeation study allows for the evaluation of drug retention in the skin, fundamental for the understanding of active agent disposition after administration. ERI should be able to cross the *stratum corneum* barrier when applied to the skin, remaining on this tissue in a suitable concentration to exhibit biological activity [4], where the adequate light wavelength is able to excite the PS. Photoacoustic spectroscopy is a helpful tool to investigate the permeation, retention and distribution of drugs in biological tissues by *in vitro*, *ex vivo* or *in vivo* tests [56,85]. This technique is based on the determination of several optical spectral of absorption by photoacoustic signals. The photoacoustic spectra obtained for the preparations in porcine skin and mucosa are displayed in Fig. 6.
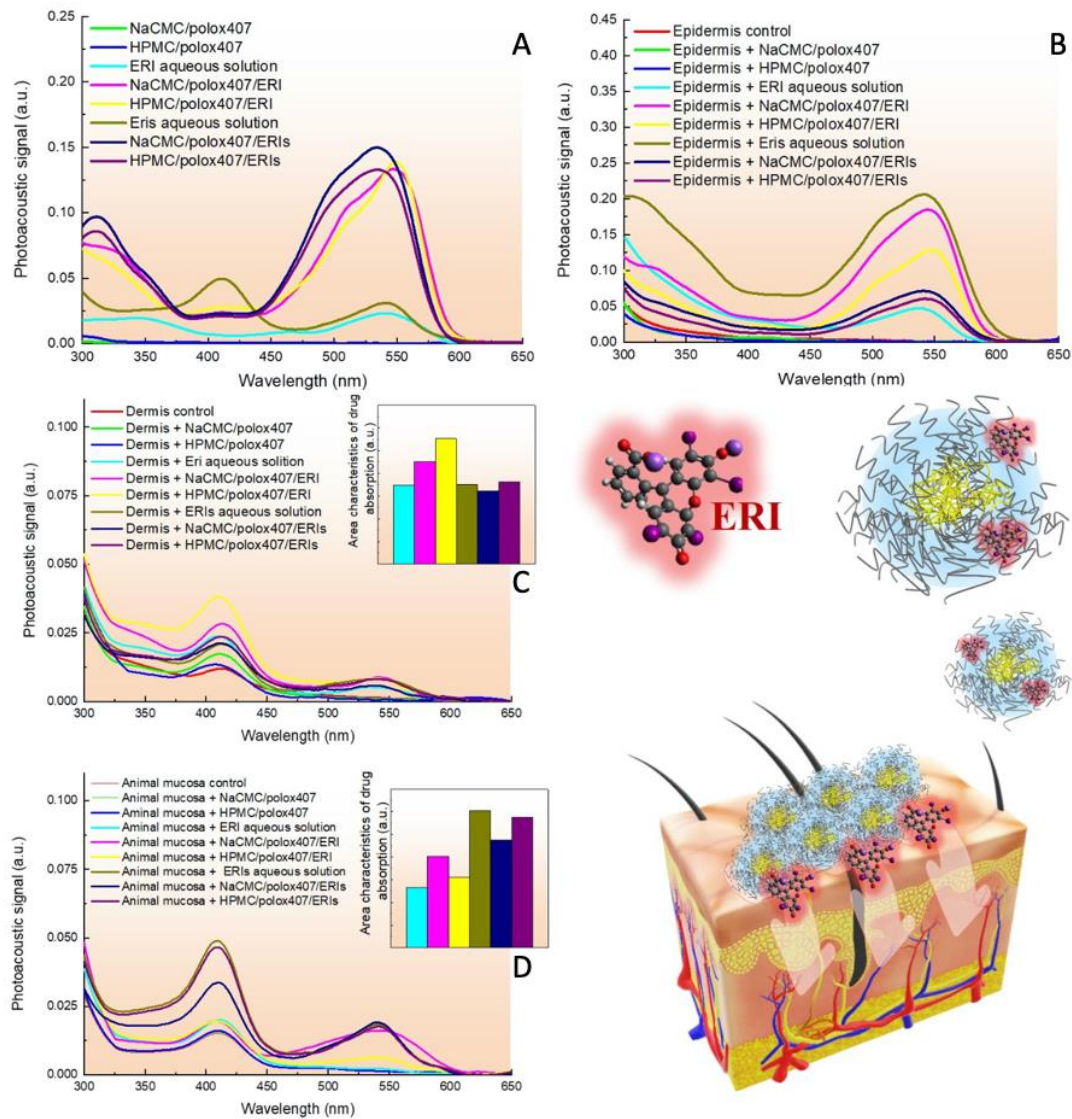
Fig. 6. Optical absorption spectra of the formulations obtained by the photoacoustic spectroscopy technique (A). Optical absorption spectra of skin permeation of at least three replicates of each formulation by the photoacoustic spectroscopy technique in Epidermis (B), Dermis (C) and Mucosa (D) with the area of absorption characteristic of drugs for the dermis and mucosa.

Fig. 6A includes the absorption spectra of all tested formulations. Raw NaCMC and HPMC did not show optic absorption at the region analyzed. Both aqueous control solution, and formulations containing ERI or ERIs demonstrated a broad band of optic absorption between 300 to 600 nm. Therefore, the detection of this signal alongside the animal tissue indicates the presence of the topically applied drug. Fig. 6B and C display the optic absorption spectrum of epidermis and dermis surface after 30 min of topical application. It is possible to observe the presence of the drug by the increase of the intensity at 300-600 nm in comparison to the skin control (Fig. 6B and C). To quantify dermis retention, the integration of the area of absorption between 300 and 650 nm was assessed (Fig. 6C).

The data demonstrate the biomedical systems were capable of releasing ERI and ERIs in a relatively short time (Fig. 6, Fig. S4, Table S5). Evaluating the dermis tissue, both ERI and ERIs reached this portion of the skin, suggesting the topical systems are promising for PS delivery. They allowed the release of both PSs along with cutaneous and mucosal diffusion effects. The study demonstrated the systems ensure efficacy when applying radiation in the green region. In the epidermis ERI attained higher concentrations after 30 minutes in comparison to ERIs when in polymeric systems, which may be related to its amphiphilic potential, contributing with its higher skin diffusion. Considering the dermis, HPMC-ERI preparation was the system that showed the highest permeation, in accordance with its high relative hydrophobicity and small size (15.5 ± 3.5 nm). It was followed by NaCMC-ERI system, HPMC-ERIs and NaCMC-ERIs systems, which agrees with the size of their micelles already reported in the literature (14.5 ± 7.3 nm, 14.4 ± 2.9 nm and 21.5 ± 9,.8 nm, respectively). Comparing the solution with drug delivery preparations, the micellar systems improved the permeation of both drugs into the dermis, suggesting their carriage through the outer skin barrier by micelles may improve their delivery to this deeper layer. Moreover, it is also believed the hydrophilic/hydrophobic balance and charge density of the mixtures may

affect their permeation profile. Even with lower bioadhesion compared to the mucoadhesion, the fast permeation of the drug in the skin may ensure its therapeutic efficacy. Nonetheless, NaCMC-ERIs system was the only preparation that presented slight reduction of permeation in comparison to the control, which may be supported by its high charger density, plus its increased micellar size previously evidenced by TEM.

Considering the mucosal tissue, ERIs reached higher permeation than ERI, with HPMC-based preparation demonstrating better performance, following the control solution. The lowest size of micellar structures found for HPMC systems may facilitate permeation and retention in both tissues. Compared to the dermis, ERI presented lower permeation in the mucosa. Since there is a higher degree of hydration, its comparatively higher hydrophobicity could make its permeation unsuited in this tissue, particularly in the presence of mucus. However, once ERI was incorporated to the micellar preparations, its permeation was higher than the aqueous solution. Although ERIs could achieve increased permeation on the mucosa, when added to the polymeric preparations its permeation was slightly impaired, since its free form may be more available to diffuse in a hydrated environment than the nanostructured system.

3.6. Evaluation of photodynamic activity

As potential drug delivery systems for photodynamic therapy, the preparations were evaluated regard their chemical photodynamic activity. Chemical dosimeters have been used to estimate the ability of the PS generating highly cytotoxic reactive oxygen species (ROS), especially singlet oxygen, when incorporated into binary polymeric systems (Fig. S8A) [4,35]. The experiments involving UA evaluate the photochemical and photophysical processes to which the PS is exposed after excitation. The absorption of photons, through the chromophore of the xanthene portion, is possible due to their adequate spectral overlap (Fig. S8B). Once this

absorption occurs, ERI and ERIs electrons are elevated to their excited state (Eri*[singlet]), where intersystem crossing (ISC, $\Phi ISC = 0.68$ in water [86]) can occur with the formation of Eri*[triplet] (Fig. S8A) [87]. The triplet state has sufficient lifetime to allow the interaction between Eri*[triplet] and neighboring molecules with the same multiplicity (e.g. molecular oxygen). Thereby, the PS can develop reactions involving the Type I mechanism, producing superoxide, peroxide or hydroxyl radicals and/or Type II, with singlet oxygen formation. The products of each type of reaction exhibit high cytotoxicity, being able to lead many microorganisms and tumoral cells to death [33,88]. Along with the assessment of photodynamic activity, the formation of these reactive species promotes the degradation of UA, consequently reducing its peak of absorption at 293 nm, as shown in Table 2 [4,33].

Table 2 shows the spectra obtained with illumination time and absorption intensity at each wavelength, during the photodynamic activity assessment. Generally, in the absence of light, the electronic absorption band of UA remains constant in the systems, since there are not products able to degrade it in the supernatant solution. However, when illuminated, the PS becomes activated and may produce ROS, which fosters UA degradation, with consequent reduction of its band at 293 nm. Besides the remarkable change in the relative peak of UA, the erosion of the polymeric systems containing ERI or ERIs may also occur, which is confirmed by the rapid increase of ERI and ERIs peaks at 528 nm, after few minutes of assay. According to the literature, the effects of erosion in hydrogels predominantly composed of polox407 depend on the nature and proportion of the polymeric mixture [89,90]. For instance, some authors have evaluated dermatological systems composed of polox407 and methylcellulose (MC) or HPMC. They attributed dissolution effects of their matrix to changes in the number and dimensions of micellar aqueous channels, linking it to the interaction between polymers, which promote variations in the viscosity of the systems [90]. Therefore, the favored dissolution of the matrix can lead to the increase of the peak at 528 nm, which is also observed

in Table 2, with ERIs-preparations presenting a larger shift after 20 min. This effect may be associated with the reorganization processes of the drug in the micellar microenvironment, as well as with its partition to the aqueous medium (molar absorption coefficient in the water at 532 nm, 9.66×10^4 L/mol/cm) [91] governed by the highly hydrophilic profile of ERIs (log kp -0.05) [50] in comparison to the amphiphilic behavior of ERI (log kp 0.46) [92].

Studies were also conducted involving the matrices in the absence of the drugs, showing the maintenance of the absorption band of UA, either in presence or absence of light (not shown). Kinetic adjustments using bi-exponential model, although frequently reported in the literature [4,59,62], were not able to fit the data. The absorption spectra of erythrosine shows, among others, main bands at 528 and 260 nm [1], with the latter extremely close to the UA peak. Hence, the low molar absorptivity and slowly increasing ERI/ERIs peak, at 260 nm [93], may blur the decreasing peak of UA, impairing the applicability of the kinetic model. Nonetheless, from the outcomes, it is possible to ensure substantial photodynamic activity, even considering the effects of the matrix dissolution and release of ERI or ERIs into the aqueous medium. These data agree with studies performed by Pellosi and collaborators, which showed satisfactory values of $\Phi_\Delta{}^1O_2$ (quantum singlet oxygen yield) for ERI in water (0.62) and into polox407 dispersions (0.64) [1].

Table 2

Evaluation of the photodynamic activity of neutral erythrosine (ERI) or disodium salt erythrosine (ERIs) comprising binary polymeric systems composed of 17.5% (w/w) poloxamer 407 (polox407) and 3% (w/w) hydroxypropyl methylcellulose (HPMC) or 1% (w/w) sodium carboxymethylcellulose (NaCMC).
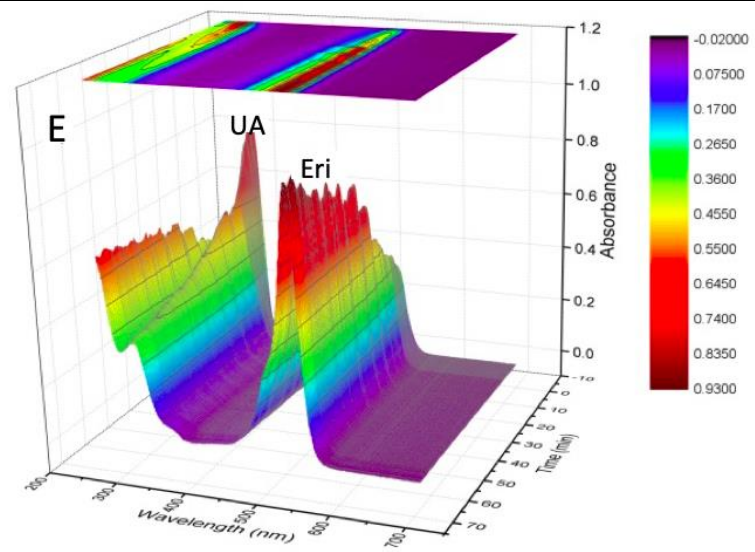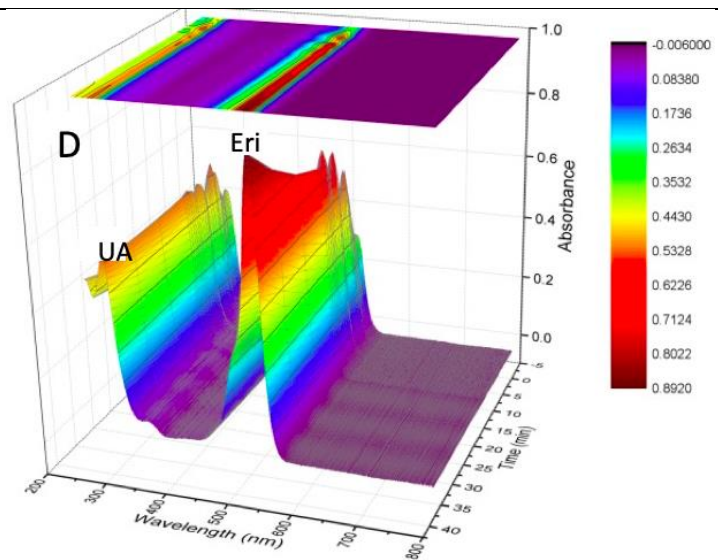
Platform	Without light	With light
polox407/HPMC/ERI		
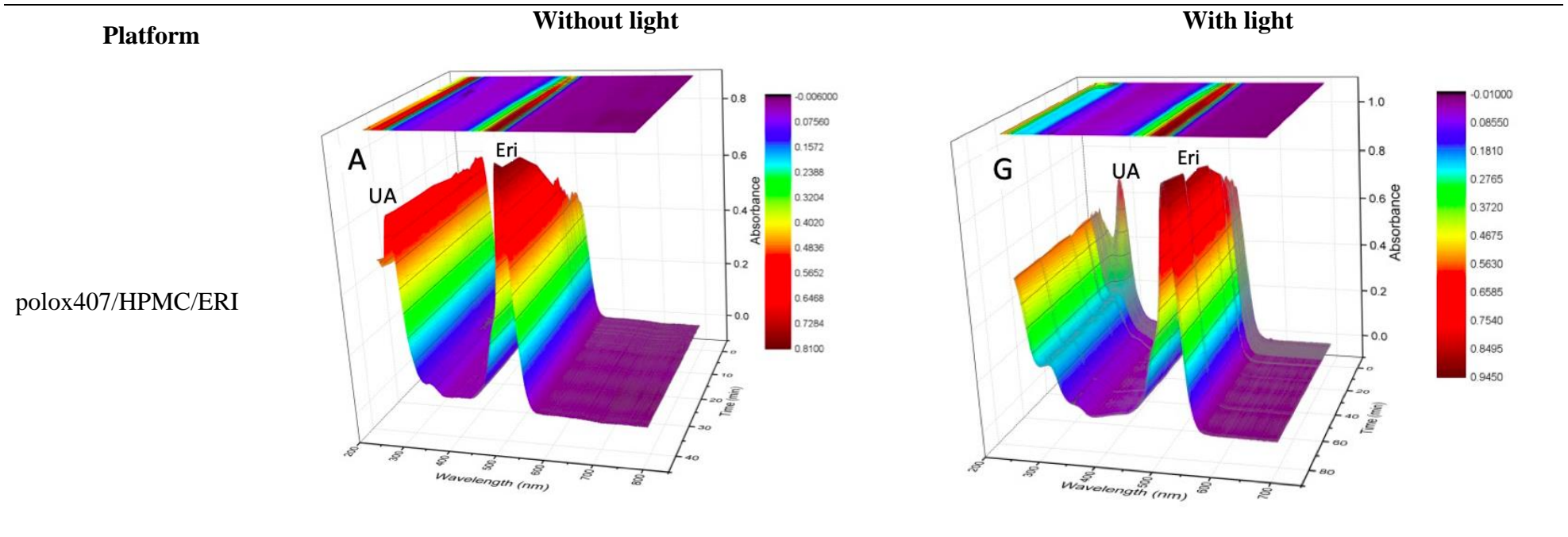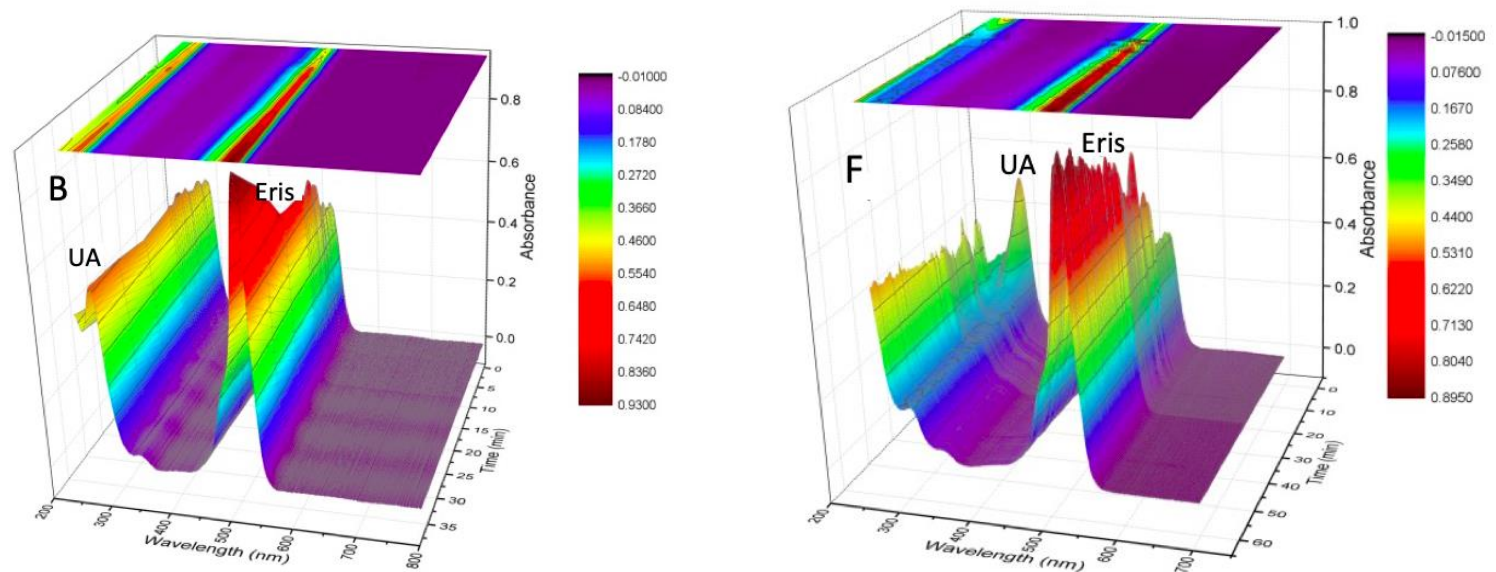
polox407/HPMC/ERIs

polox407/NaCMC/ERI
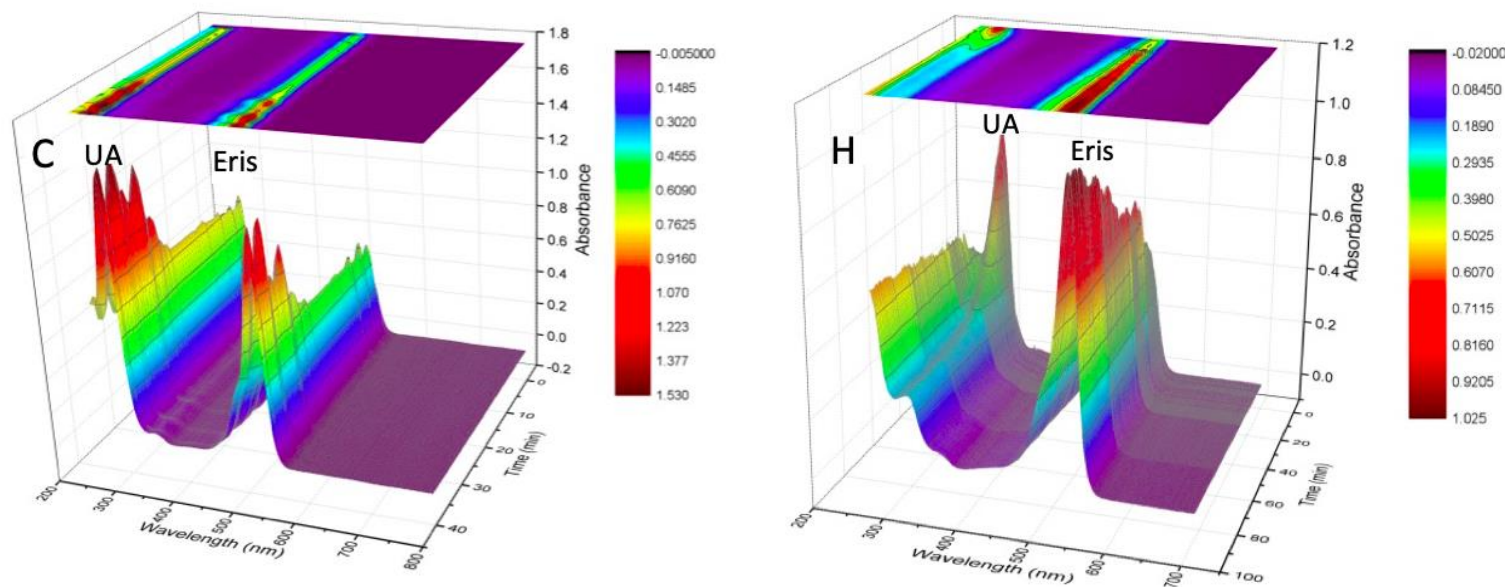
polox407/NaCMC/ERIs

3.7. Phototoxicity assay

Considering the potential photodynamic activity of the polymer systems containing ERI and ERIs, their phototoxicity were evaluated using non-tumoral murine fibroblasts (Balb/3T3, Fig. 7) and tumoral melanoma cells (B16-F10, Fig. 8). PDT has been reported to change cell signaling and metabolism through some pathways, leading to cell death by apoptosis or necrosis. The type of photodamage is linked to the subcellular localization of the PS within the cell. PS diffusion across the cellular membrane is dependent both on ionic charges and the partition coefficient between aqueous and lipophilic phases (log P) properties of each PS system [84].
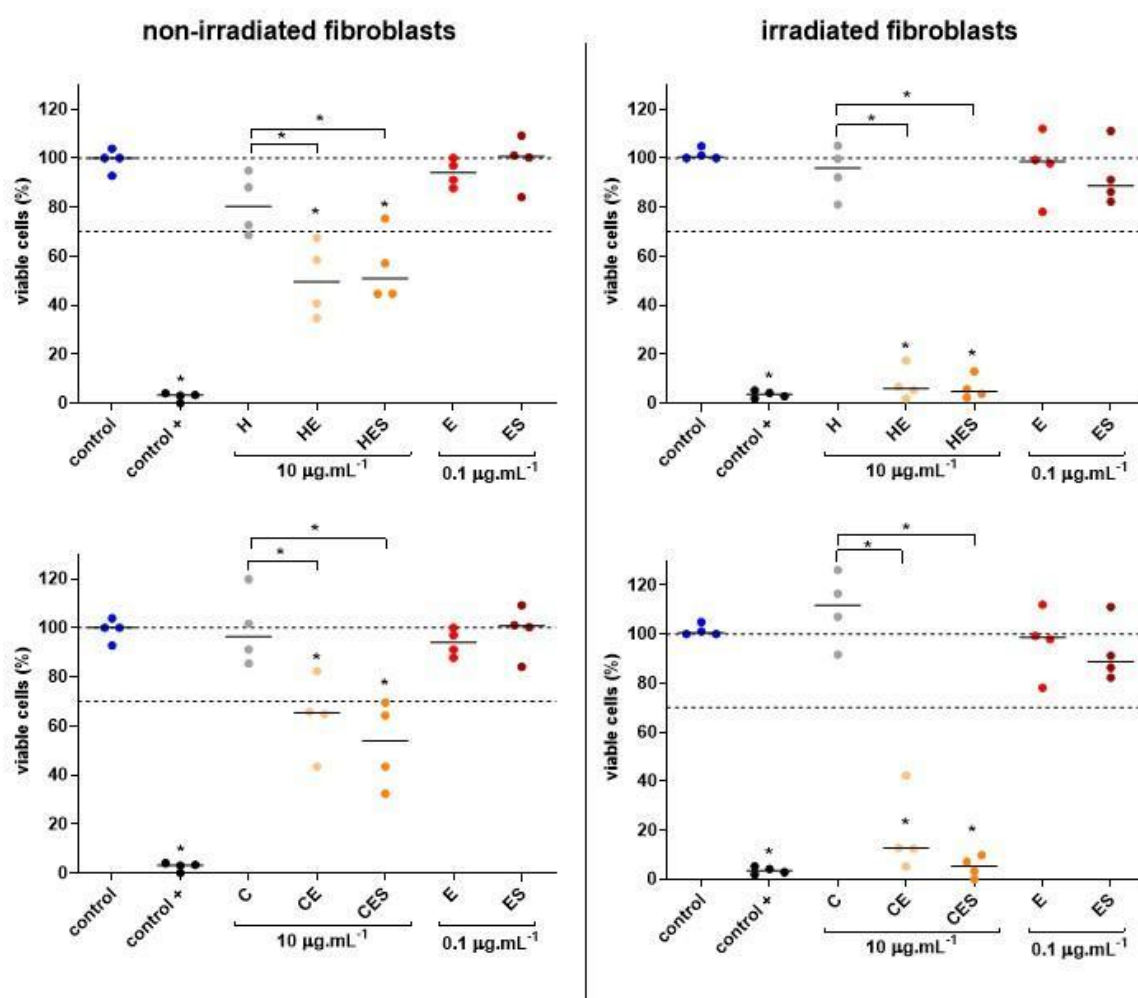

Fig. 7. Cytotoxicity and phototoxicity of the preparations in non-tumoral murine fibroblasts. Polymer systems were kept at 10 μg/mL, containing 0.1 μg/mL of ERI/ ERIs and, ERI and

ERIs solutions were evaluated at the same concentration (0.1 µg/mL). Results were from four independent experiments performed in technical quadruplicate with the line showing the medians of the independent experiments. * Results statistically significative ($p < 0.05$) using Mann-Whitney non-parametric test. Dotted lines show the interval of 0–30% reduction of cell viability [91]. Preparations composed of poloxamer 407 and hydroxypropyl methylcellulose (H), with neutral erythrosine (HE) or disodium salt erythrosine (HES); poloxamer 407 and sodium carboxymethylcellulose (C), with neutral erythrosine (CE) or disodium salt erythrosine (CES); neutral erythrosine solution (E) and disodium salt erythrosine solution (ES).

The control represents cells without treatment, which defined a median of 100% viability. The outcomes show that polymer systems without erythrosine were biocompatible, since the fibroblast viability was not reduced, even under light exposure (Fig. 7). On the other hand, erythrosine-loaded systems decreased the fibroblasts viability by around 50% and 40% for HPMC and NaCMC preparations, respectively. When exposed to the suitable light wavelength (Fig. 7B), both polymeric systems - containing ERI or ERIs - exhibited high photodynamic activity, decreasing cell viability to around 5%. Interestingly, pure erythrosine (in both at neutral or salt form) did not affect the cell viability even after light irradiation (Fig. 7). This behavior is probably linked to the self-aggregation state of the PS when into aqueous solutions [21].
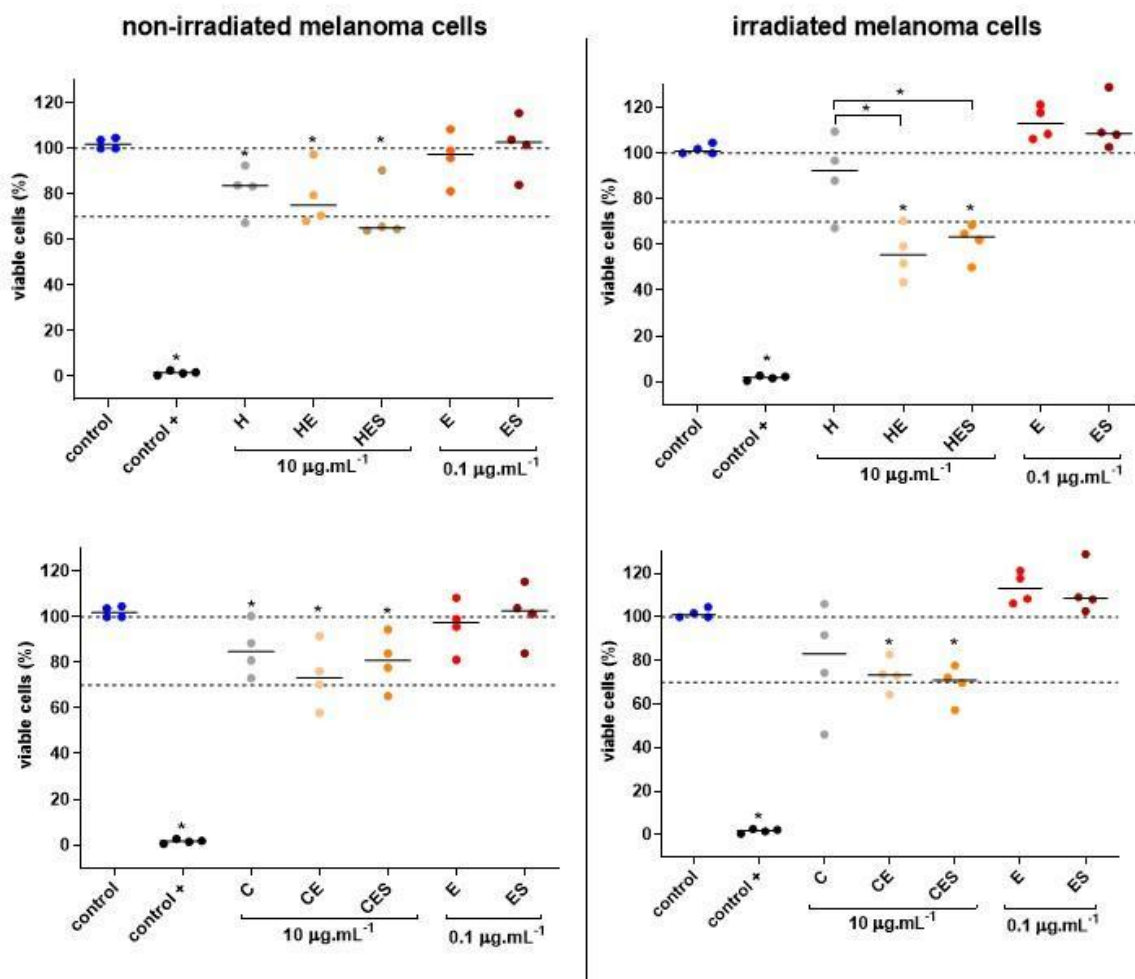
Fig. 8. Cytotoxicity and phototoxicity of the preparations in melanoma tumor cell. Polymer systems were kept at 10 μg/mL, containing 0.1 μg/mL of ERI/ ERIs and, ERI and ERIs solutions were evaluated at the same concentration (0.1 μg/mL). Results were from four independent experiments performed in technical quadruplicate and the line showed the medians of the independent experiments. * Results statistically significative ($p < 0.05$) using Mann-Whitney non-parametric test. Dotted lines show the interval of 0–30% reduction of cell viability [91]. Preparations composed of poloxamer 407 and hydroxypropyl methylcellulose (H), with neutral erythrosine (HE) or disodium salt erythrosine (HES); poloxamer 407 and sodium carboxymethylcellulose (C), with neutral erythrosine (CE) or disodium salt erythrosine (CES); neutral erythrosine solution (E) and disodium salt erythrosine solution (ES).

The potential antitumoral phototoxic activity of the erythrosine, incorporated into the polymeric systems, was evaluated against melanoma tumor cells (Fig. 8). The melanoma cells treated with erythrosine-loaded polymeric systems showed around 65% to 83% viability relative to control (Fig. 8). Even though this cell viability reduction was statistically significant ($p<0.05$), it could be classified as a non- to moderately- cytotoxic product according to ISO 10993-5 [94,95]. When exposed to light, the viability of the melanoma cells treated with both PS loaded-polymeric systems decreased by around 30-40% (Fig. 8). There were no differences considering the effect of erythrosine-type loaded into the systems. However, among all the tested systems the HPMC loaded with the ERI form (HE) showed an improved performance against the melanoma cell line (Fig. 8), as well as the highest dermis permeation among the systems, as mentioned previously. Comparing the melanoma cell viability treated with HE, before and after the light exposure, it is possible to detect a greater decrease of cell viability after the light exposure ($p < 0.05$). Interestingly, this behavior was not observed among the other binary polymeric preparations (Fig. S9).

Furthermore, as also observed in non-tumoral fibroblasts, melanoma cells were not affected by pure erythrosine (ERI or ERIs), even after light exposure (Fig. 8). The observed phototoxic biological effect corroborated that the log P of the drug may impair their photodynamic mechanism of action. When they were incorporated into the micellar system, both ERI and ERIs were able to significantly reduce healthy and tumor cell viability, mainly in presence of light (Fig. S9), whilst preparations without drug or solutions containing only the PS were not able to do the same (Fig. S10). Hence, the micelles were able to boost photodynamic activity of ERI and ERIs, facilitating their interaction with biological membranes. Although some poloxamers have been reported to present some tendency to cause cell damage, copolymers of polox407, with PPO = 3.6 kDa, have presented low cytotoxicity in certain cell lines (Caco-2 and HMEC-1) [96]. Moreover, topical application is considered to be

relatively low risk as a route of administration due to the presence of epithelial barriers such as the Stratum Corneum.

Despite the systems presenting an elevated cytotoxicity for the healthy fibroblasts, the selectivity of the systems against the tumor cells may be achieved by the topical application of the thermoresponsive and mucoadhesive formulations. The mechanical, rheological, and adhesive properties of the systems contribute to their local retention after the local application. Further studies have to be performed varying drug concentration and/or time of light exposition, in order to understand the photodynamic therapy of ERI/ERIs against melanoma cell line. However, it is feasible the structuration and size micelles may have important bearing with the activity against melanoma cells, since HPMC-ERI system have already demonstrated improved interaction among its constituents, small micelle size [23] and high skin permeation.

4. Conclusion

Polymeric blends composed of polox407 and HPMC or NaCMC were developed and characterized for ERI or ERIs delivery with good performance in photodynamic therapy. The rheological characterization of the formulations demonstrated pseudoplastic behavior, with ERI or ERIs, affecting yield value. All systems presented thixotropic and viscoelastic properties at 37 °C, with suitable $T_{sol/gel}$ for topical use. The mechanical properties were suitable for application, with improved softness index for systems containing drug. Bio/mucoadhesion performance was efficient for all the evaluated systems, displaying improved adhesion to the mucosa in contrast to the skin. *Ex vivo* assays showed the systems could release and deliver both PSs, reaching different layers of the skin and mucosa. Despite the differences observed on the structuring and characterization of the systems containing ERI or ERIs, all formulations composed of 17.5% (w/w) polox407 and 3% (w/w) HPMC or 1% (w/w) NaCMC with 1% (w/w) ERI or ERIs produced sufficient *in vitro* cytotoxic species in non-tumoral cell culture

phototoxicity assay. However, the polox407/HPMC/ERI system keen interest against melanoma cell line, with important phototoxic outcomes in line with its characterization. Therefore, it was possible to conclude the functional micelles composed of thermoresponsive and mucoadhesive polymers could boost the photodynamic activity of ERI and ERIs, improving the delivery of both PSs to the cells.

Data availability

Data will be made available on request.

Acknowledgments

References

[1]   D.S. Pellosi, B.M. Estevão, C.F. Freitas, T.M. Tsubone, W. Caetano, N. Hioka, Photophysical properties of erythrosin ester derivatives in ionic and non-ionic micelles, Dye. Pigment. 99 (2013) 705–712. doi:10.1016/j.dyepig.2013.06.026.

[2]   M.C. DeRosa, R.J. Crutchley, Photosensitized singlet oxygen and its applications, Coord. Chem. Rev. 233–234 (2002) 351–371. doi:10.1016/S0010-8545(02)00034-6.

[3]   A.C.B.P. Costa, V.M. De Campos Rasteiro, C.A. Pereira, E.S.H. Da Silva Hashimoto, M. Beltrame, J.C. Junqueira, A.O.C. Jorge, Susceptibility of Candida albicans and

Candida dubliniensis to erythrosine- and LED-mediated photodynamic therapy, Arch. Oral Biol. 56 (2011) 1299–1305. doi:10.1016/j.archoralbio.2011.05.013.

[4]   K. da S.S. Campanholi, G. Braga, J.B. da Silva, N.L. da Rocha, L.M.B. de Francisco, É.L. de Oliveira, M.L. Bruschi, L. V. de Castro-Hoshino, F. Sato, N. Hioka, W. Caetano, Biomedical Platform Development of a Chlorophyll-Based Extract for Topic Photodynamic Therapy: Mechanical and Spectroscopic Properties, Langmuir. 34 (2018) 8230–8244. doi:10.1021/acs.langmuir.8b00658.

[5]   E. Munin, L.M. Giroldo, L.P. Alves, M.S. Costa, Study of germ tube formation by Candida albicans after photodynamic antimicrobial chemotherapy (PACT), J. Photochem. Photobiol. B Biol. 88 (2007) 16–20. doi:10.1016/j.jphotobiol.2007.04.011.

[6]   D.E.J.G.J. Dolmans, D. Fukumura, R.K. Jain, Photodynamic therapy for cancer, Nat. Rev. Cancer. 3 (2003) 375–380. doi:10.1038/nrc1070.

[7]   L. Dong, X. Li, X. Shen, W. Zhang, J. Zhang, Y. Wang, Y. Lu, Efficacy and safety of 5-aminolevulinic acid photodynamic therapy for the treatment of ulcerative squamous cell carcinoma, Photodiagnosis Photodyn. Ther. 30 (2020) 101710. doi:10.1016/j.pdpdt.2020.101710.

[8]   K.H. Nelke, W. Pawlak, J. Leszczyszyn, H. Gerber, Photodynamic therapy in head and neck cancer, Postepy Hig. Med. Dosw. 68 (2014) 119–128. doi:10.5604/17322693.1088044.

[9]   G. Yin, Y. Zhang, M. Geng, B. Cai, Y. Zheng, Cure of condyloma acuminata covering the glans penis using aminolevulinic acid/photodynamic therapy, Photodiagnosis Photodyn. Ther. 30 (2020) 101658. doi:10.1016/j.pdpdt.2020.101658.

[10]   M.A. Biel, Photodynamic therapy and the treatment of head and neck neoplasia, Laryngoscope. 108 (1998) 1259–1268. doi:10.1097/00005537-199809000-00001.

[11]   G. Garcia de Carvalho, J.C. Sanchez-Puetate, N. Casalle, E. Marcantonio Junior, D. Leal Zandim-Barcelos, Antimicrobial photodynamic therapy associated with bone regeneration for peri-implantitis treatment: A case report, Photodiagnosis Photodyn. Ther. 30 (2020) 101705. doi:10.1016/j.pdpdt.2020.101705.

[12]   A.L.P. Silvestre, A.M. dos Santos, A.B. de Oliveira, T.M. Ferrisse, F.L. Brighenti, A.B. Meneguin, M. Chorilli, Evaluation of photodynamic therapy on nanoparticles and films loaded-nanoparticles based on chitosan/alginate for curcumin delivery in oral biofilms, Int. J. Biol. Macromol. 240 (2023). doi:10.1016/j.ijbiomac.2023.124489.

[13]   A.C.B.P. Costa, V.M. Campos Rasteiro, E.S.H. Da Silva Hashimoto, C.F. Araújo, C.A. Pereira, J.C. Junqueira, A.O.C. Jorge, Effect of erythrosine- and LED-mediated photodynamic therapy on buccal candidiasis infection of immunosuppressed mice and Candida albicans adherence to buccal epithelial cells, Oral Surg. Oral Med. Oral Pathol. Oral Radiol. 114 (2012) 67–74. doi:10.1016/j.oooo.2012.02.002.

[14] D. Cao, W. Zhu, Y. Kuang, S. Zhao, A safe and effective treatment: Surgery combined with photodynamic therapy for multiple basal cell carcinomas, Photodiagnosis Photodyn. Ther. 28 (2019) 133–135. doi:10.1016/j.pdpdt.2019.09.001.

[15] M. Zamani, M. Aghajanzadeh, S. Jashnani, S.S. Shahangian, F. Shirini, Hyaluronic acid coated spinel ferrite for combination of chemo and photodynamic therapy: Green synthesis, characterization, and in vitro and in vivo biocompatibility study, Int. J. Biol. Macromol. 219 (2022) 709–720. doi:10.1016/j.ijbiomac.2022.08.036.

[16] S. Wood, D. Metcalf, D. Devine, C. Robinson, Erythrosine is a potential photosensitizer for the photodynamic therapy of oral plaque biofilms, J. Antimicrob. Chemother. 57 (2006) 680–684. doi:10.1093/jac/dkl021.

[17] A.D. Garg, M. Bose, M.I. Ahmed, W.A. Bonass, S.R. Wood, In vitro studies on erythrosine-based photodynamic therapy of malignant and pre-malignant oral epithelial cells, PLoS One. 7 (2012) 1–12. doi:10.1371/journal.pone.0034475.

[18] L.M. Tokubo, P.L. Rosalen, J. de Cássia Orlandi Sardi, I.A. Freires, M. Fujimaki, J.E. Umeda, P.M. Barbosa, G.O. Tecchio, N. Hioka, C.F. de Freitas, R.S. Suga Terada, Antimicrobial effect of photodynamic therapy using erythrosine/methylene blue combination on Streptococcus mutans biofilm, Photodiagnosis Photodyn. Ther. 23 (2018) 94–98. doi:10.1016/j.pdpdt.2018.05.004.

[19] C. Garapati, B. Clarke, S. Zadora, C. Burney, B.D. Cameron, R. Fournier, R.F. Baugh, S.H.S. Boddu, Development and characterization of erythrosine nanoparticles with potential for treating sinusitis using photodynamic therapy, Photodiagnosis Photodyn. Ther. 12 (2015) 9–18. doi:10.1016/j.pdpdt.2015.01.005.

[20] K. Plaetzer, T. Kiesslich, T. Verwanger, B. Krammer, The modes of cell death induced by PDT: An overview, Med. Laser Appl. 18 (2003) 7–19. doi:10.1078/1615-1615-00082.

[21] C.F. de Freitas, M.C. Montanha, D.S. Pellosi, E. Kimura, W. Caetano, N. Hioka, "Biotin-targeted mixed liposomes: A smart strategy for selective release of a photosensitizer agent in cancer cells," Mater. Sci. Eng. C. 104 (2019) 109923. doi:10.1016/j.msec.2019.109923.

[22] C.F. de Freitas, D. Vanzin, T.L. Braga, D.S. Pellosi, V.R. Batistela, W. Caetano, N. Hioka, Multivariate analysis of protolytic and tautomeric equilibria of Erythrosine B and its ester derivatives in ionic and non-ionic micelles, J. Mol. Liq. 313 (2020) 113320. doi:10.1016/j.molliq.2020.113320.

[23] J. Bassi da Silva, K. da Silva Souza Campanholi, G. Braga, P.R. de Souza, W. Caetano, M.T. Cook, M.L. Bruschi, The effect of erythrosine-B on the structuration of poloxamer 407 and cellulose derivative blends: In silico modelling supporting experimental studies, Mater. Sci. Eng. C. 130 (2021). doi:10.1016/j.msec.2021.112440.

[24] C.F. de Freitas, N.L. da Rocha, I.S. Pereverzieff, V.R. Batistela, L.C. Malacarne, N.

Hioka, W. Caetano, Potential of triblock copolymers Pluronic® P-84 and F-108 with erythrosine B and its synthetic ester derivatives for photodynamic applications, J. Mol. Liq. 322 (2021) 114904. doi:10.1016/j.molliq.2020.114904.

[25] A.M. Bodratti, P. Alexandridis, Amphiphilic block copolymers in drug delivery: advances in formulation structure and performance, Expert Opin. Drug Deliv. 15 (2018) 1085–1104. doi:10.1080/17425247.2018.1529756.

[26] M.L. Veyries, G. Couarraze, S. Geiger, F. Agnely, L. Massias, B. Kunzli, F. Faurisson, B. Rouveix, Controlled release of vancomycin from Poloxamer 407 gels, Int. J. Pharm. 192 (1999) 183–193. doi:10.1016/S0378-5173(99)00307-5.

[27] R.M. Nalbandian, R.L. Henry, H.S. Wilks, Artifical skin. II. Pluronic F-127 silver nitrate or silver lactate gel in the treatment of thermal burns, J. Biomed. Mater. Res. 6 (1972) 583–590. doi:10.1002/jbm.820060610.

[28] P. Alexandridis, T. Alan Hatton, Poly(ethylene oxide)poly(propylene oxide)poly(ethylene oxide) block copolymer surfactants in aqueous solutions and at interfaces: thermodynamics, structure, dynamics, and modeling, Colloids Surfaces A Physicochem. Eng. Asp. 96 (1995) 1–46. doi:10.1016/0927-7757(94)03028-X.

[29] S. Samanta, D. Roccatano, Interaction of curcumin with PEO-PPO-PEO block copolymers: A molecular dynamics study, J. Phys. Chem. B. 117 (2013) 3250–3257. doi:10.1021/jp309476u.

[30] F.B. Borghi-Pangoni, M.V. Junqueira, S.B. de Souza Ferreira, L.L. Silva, B.R. Rabello, L.V. de Castro, M.L. Baesso, A. Diniz, W. Caetano, M.L. Bruschi, Preparation and characterization of bioadhesive system containing hypericin for local photodynamic therapy, Photodiagnosis Photodyn. Ther. 19 (2017) 284–297. doi:10.1016/j.pdpdt.2017.06.016.

[31] M.A. Abou-Shamat, J. Calvo-Castro, J.L. Stair, M.T. Cook, Modifying the Properties of Thermogelling Poloxamer 407 Solutions through Covalent Modification and the Use of Polymer Additives, Macromol. Chem. Phys. 220 (2019) 1–19. doi:10.1002/macp.201900173.

[32] G. Ulbricht, W. Hoffman, H. Wanka, Phase Diagrams and Aggregation Behavior of Poly(oxyethy1ene)-Poly (oxypropylene)-Poly(oxyethylene) Triblock Copolymers in Aqueous Solutions, Macromolecules. 27 (1994) 4145–4159.

[33] K. da Silva Souza Campanholi, J.M. Jaski, R.C. da Silva Junior, A.B. Zanqui, D. Lazarin-Bidóia, C.M. da Silva, E.A. da Silva, N. Hioka, C.V. Nakamura, L. Cardozo-Filho, W. Caetano, Photodamage on Staphylococcus aureus by natural extract from Tetragonia tetragonoides (Pall.) Kuntze: Clean method of extraction, characterization and photophysical studies, J. Photochem. Photobiol. B Biol. (2020). doi:10.1016/j.jphotobiol.2019.111763.

[34] M. V. Junqueira, F.B. Borghi-Pangoni, S.B.S. Ferreira, B.R. Rabello, N. Hioka, M.L.

Bruschi, Functional Polymeric Systems as Delivery Vehicles for Methylene Blue in Photodynamic Therapy, Langmuir. 32 (2016) 19–27. doi:10.1021/acs.langmuir.5b02039.

[35] F.B. Borghi-Pangoni, M.V. Junqueira, S.B. de Souza Ferreira, L.L. Silva, B.R. Rabello, W. Caetano, A. Diniz, M.L. Bruschi, Screening and In Vitro Evaluation of Mucoadhesive Thermoresponsive System Containing Methylene Blue for Local Photodynamic Therapy of Colorectal Cancer, Pharm. Res. (2015). doi:10.1007/s11095-015-1826-8.

[36] D. Szweda, R. Szweda, A. Dworak, B. Trzebicka, Thermoresponsive poly[oligo(ethylene glycol) methacrylate]s and their bioconjugates - Synthesis and solution behavior, Polimery/Polymers. 62 (2017) 298–310. doi:10.14314/polimery.2017.298.

[37] S.B. De Souza Ferreira, J.B. Da Silva, F.B. Borghi-Pangoni, M.V. Junqueira, M.L. Bruschi, Linear correlation between rheological, mechanical and mucoadhesive properties of polycarbophil polymer blends for biomedical applications, J. Mech. Behav. Biomed. Mater. 68 (2017). doi:10.1016/j.jmbbm.2017.02.016.

[38] S.B. De Souza Ferreira, T.D. Moço, F.B. Borghi-Pangoni, M.V. Junqueira, M.L. Bruschi, Rheological, Mucoadhesive and Textural Properties of Thermoresponsive Polymer Blends for Biomedical Applications, J. Mech. Behav. Biomed. Mater. 55 (2015) 164–178. doi:10.1016/j.jmbbm.2015.10.026.

[39] S. Barbosa, D.S. Ferreira, J.B. da Silva, M. Volpato, F.B. Borghi-pangoni, R. Guttierres, M. Luciano, The importance of the relationship between mechanical analyses and rheometry of mucoadhesive thermoresponsive polymeric materials for biomedical applications, J. Mech. Behav. Biomed. Mater. (2017). doi:10.1016/j.jmbbm.2017.05.040.

[40] M.L. Bruschi, D.S. Jones, H. Panzeri, M.P.D. Gremião, O. De Freitas, E.H.G. Lara, Semisolid systems containing propolis for the treatment of periodontal disease: In vitro release kinetics, syringeability, rheological, textural, and mucoadhesive properties, J. Pharm. Sci. 96 (2007) 2074–2089. doi:10.1002/jps.20843.

[41] D.S. Jones, M.L. Bruschi, O. de Freitas, M.P.D. Gremião, E.H.G. Lara, G.P. Andrews, Rheological, mechanical and mucoadhesive properties of thermoresponsive, bioadhesive binary mixtures composed of poloxamer 407 and carbopol 974P designed as platforms for implantable drug delivery systems for use in the oral cavity, Int. J. Pharm. 372 (2009) 49–58. doi:10.1016/j.ijpharm.2009.01.006.

[42] W. Wang, P.C.L. Hui, E. Wat, F.S.F. Ng, C.W. Kan, X. Wang, E.C.W. Wong, H. Hu, B. Chan, C.B.S. Lau, P.C. Leung, In vitro drug release and percutaneous behavior of poloxamer-based hydrogel formulation containing traditional Chinese medicine, Colloids Surfaces B Biointerfaces. 148 (2016) 526–532.

doi:10.1016/j.colsurfb.2016.09.036.

[43] C. Pagano, S. Giovagnoli, L. Perioli, M.C. Tiralti, M. Ricci, Development and characterization of mucoadhesive-thermoresponsive gels for the treatment of oral mucosa diseases, Eur. J. Pharm. Sci. 142 (2020) 105125. doi:10.1016/j.ejps.2019.105125.

[44] J.B. da Silva, M.T. Cook, M.L. Bruschi, Thermoresponsive systems composed of poloxamer 407 and HPMC or NaCMC: mechanical, rheological and sol-gel transition analysis, Carbohydr. Polym. 240 (2020). doi:10.1016/j.carbpol.2020.116268.

[45] J.B. da Silva, R.S. dos Santos, M.B. da Silva, G. Braga, M.T. Cook, M.L. Bruschi, Interaction between mucoadhesive cellulose derivatives and Pluronic F127: Investigation on the micelle structure and mucoadhesive performance, Mater. Sci. Eng. C. 119 (2021). doi:10.1016/j.msec.2020.111643.

[46] D.S. Jones, A.D. Woolfson, J. Djokic, Texture profile analysis of bioadhesive polymeric semisolids: Mechanical characterization and investigation of interactions between formulation components, J. Appl. Polym. Sci. 61 (1996) 2229–2234. doi:10.1002/(SICI)1097-4628(19960919)61:12.

[47] H. Hägerström, K. Edsman, Interpretation of mucoadhesive properties of polymer, (2001) 1589–1599. doi:10.1211/0022357011778197.

[48] A. Chowhan, T.K. Giri, Polysaccharide as renewable responsive biopolymer for in situ gel in the delivery of drug through ocular route, Int. J. Biol. Macromol. 150 (2020) 559–572. doi:10.1016/j.ijbiomac.2020.02.097.

[49] National Library of Medicine HSDB Database, Erythrosine B, (2013) 2–4.

[50] National Library of Medicine HSDB Database, Erythrosine sodium, 27873 (2020). https://toxnet.nlm.nih.gov/cgi-bin/sis/search/a?dbs+hsdb:@term+@DOCNO+7974.

[51] I.R. Schmolka, Artificial skin I. Preparation and properties of Pluronic F127 Gels for treatment of burns, J. Biomed. MAter. Res. 6 (1972) 571–582. doi:10.1002/jbm.820060609.

[52] J. Bassi da Silva, V. V Khutoryanskiy, M.L. Bruschi, M.T. Cook, A mucosa-mimetic material for the mucoadhesion testing of thermogelling semi-solids, Int. J. Pharm. 528 (2017) 586–594. doi:10.1016/j.ijpharm.2017.06.025.

[53] L.M.B. de Francisco, H.C. Rosseto, L. de Alcântara Sica de Toledo, R.S. dos Santos, S.B. de Souza Ferreira, M.L. Bruschi, Organogel composed of poloxamer 188 and passion fruit oil: Sol-gel transition, rheology, and mechanical properties, J. Mol. Liq. 289 (2019). doi:10.1016/j.molliq.2019.111170.

[54] T.. Hemphill, W.. Campos, A. Pilehvari, Yield-power law model more accurately predicts mud rheology, Oil Gas J. 91 (1993) 45–50. https://www.ogj.com/home/article/17223447/yieldpower-law-model-more-accurately-

predicts-mud-rheology.

[55] A. Rosencwaig, A. Gersho, Theory of the photoacoustic effect with solids, J. Appl. Phys. 47 (1976) 64–69. doi:10.1063/1.322296.

[56] M.L. Baesso, J. Shen, R.D. Snook, Laser-induced photoacoustic signal phase study of stratum corneum and epidermis, Analyst. 119 (1994) 561–562. doi:10.1039/AN9941900561.

[57] F.Q. Ames, F. Sato, L.V. de Castro, L.L.M. de Arruda, B.A. da Rocha, R.K.N. Cuman, M.L. Baesso, C.A. Bersani-Amado, Evidence of anti-inflammatory effect and percutaneous penetration of a topically applied fish oil preparation : A ... Evidence of anti-inflammatory effect and percutaneous penetration of a topically applied fish oil preparation : a photoacoustic spectrosc, J. Biomed. Opt. (2017). doi:10.1117/1.JBO.22.5.055003.

[58] B.R. Rabello, A.P. Gerola, D.S. Pellosi, A.L. Tessaro, J.L. Aparício, W. Caetano, N. Hioka, Singlet oxygen dosimetry using uric acid as a chemical probe: Systematic evaluation, J. Photochem. Photobiol. A Chem. 238 (2012) 53–62. doi:10.1016/j.jphotochem.2012.04.012.

[59] B. Rabello, W. Caetano, Light dosimetry effectively absorbed (Dabs) by methylene blue in photosensitization processes employing polychromatic light sources, Quim. Nova. 41 (2018) 920–925. doi:10.21577/0100-4042.20170243.

[60] F. Fischer, G. Graschew, H.J. Sinn, W. Maier-Borst, W.J. Lorenz, P.M. Schlag, A chemical dosimeter for the determination of the photodynamic activity of photosensitizers, Clin. Chim. Acta. 274 (1998) 89–104. doi:10.1016/S0009-8981(98)00045-X.

[61] W. Wang, W. Zhang, H. Sun, Q. Du, J. Bai, X. Ge, C. Li, Enhanced photodynamic efficiency of methylene blue with controlled aggregation state in silica-methylene bule-acetate@tannic acid-iron(III) ions complexes, Dye. Pigment. (2019). doi:10.1016/j.dyepig.2018.08.068.

[62] A.P.J. Maestrin, A.C. Tedesco, C.R. Neri, M.E.F. Gandini, O.A. Serra, Y. Iamamoto, Synthesis, spectroscopy and photosensitizing properties of hydroxynitrophenylporphyrins, J. Braz. Chem. Soc. 15 (2004) 708–713. doi:Doi 10.1590/S0103-50532004000500016.

[63] G. Fotakis, J.A. Timbrell, In vitro cytotoxicity assays: Comparison of LDH, neutral red, MTT and protein assay in hepatoma cell lines following exposure to cadmium chloride, Toxicol. Lett. 160 (2006) 171–177. doi:10.1016/j.toxlet.2005.07.001.

[64] M.J. Lucero, C. Ferris, C.A. Sánchez-Gutiérrez, M.R. Jiménez-Castellanos, M. V. De-Paz, Novel aqueous chitosan-based dispersions as efficient drug delivery systems for topical use. Rheological, textural and release studies, Carbohydr. Polym. 151 (2016) 692–699. doi:10.1016/j.carbpol.2016.06.006.

[65] E. Baloglu, S.Y. Karavana, Z.A. Senyigit, T. Guneri, Rheological and mechanical properties of poloxamer mixtures as a mucoadhesive gel base, Pharm. Dev. Technol. 16 (2011) 627–636. doi:10.3109/10837450.2010.508074.

[66] J. Yun Chang, Y.K. Oh, H. Soo Kong, E. Jung Kim, D. Deuk Jang, K. Taek Nam, C.K. Kim, Prolonged antifungal effects of clotrimazole-containing mucoadhesive thermosensitive gels on vaginitis, J. Control. Release. 82 (2002) 39–50. doi:10.1016/S0168-3659(02)00086-X.

[67] M. Zhang, M. Djabourov, C. Bourgaux, K. Bouchemal, Nanostructured fluids from pluronic® mixtures, Int. J. Pharm. 454 (2013) 599–610. doi:10.1016/j.ijpharm.2013.01.043.

[68] K. Al Khateb, E.K. Ozhmukhametova, M.N. Mussin, S.K. Seilkhanov, T.K. Rakhypbekov, W.M. Lau, V. V. Khutoryanskiy, In situ gelling systems based on Pluronic F127/Pluronic F68 formulations for ocular drug delivery, Int. J. Pharm. 502 (2016) 70–79. doi:10.1016/j.ijpharm.2016.02.027.

[69] M. Dewan, B. Bhowmick, G. Sarkar, D. Rana, M.K. Bain, M. Bhowmik, D. Chattopadhyay, Effect of methyl cellulose on gelation behavior and drug release from poloxamer based ophthalmic formulations, Int. J. Biol. Macromol. 72 (2015) 706–710. doi:10.1016/j.ijbiomac.2014.09.021.

[70] L.G. Weaver, R. Stockmann, A. Postma, S.H. Thang, Multi-responsive (diethylene glycol)methyl ether methacrylate (DEGMA)-based copolymer systems, RSC Adv. 6 (2016) 90923–90933. doi:10.1039/c6ra14425j.

[71] K. Edsman, J. Carlfors, R. Petersson, Rheological evaluation of poloxamer as an in situ gel for ophthalmic use, Eur. J. Pharm. Sci. 6 (1998) 105–112. doi:10.1016/S0928-0987(97)00075-4.

[72] P.K. Sharma, S.R. Bhatia, Effect of anti-inflammatories on Pluronic® F127: Micellar assembly, gelation and partitioning, Int. J. Pharm. 278 (2004) 361–377. doi:10.1016/j.ijpharm.2004.03.029.

[73] M.T. Cook, P. Haddow, S.B. Kirton, W.J. McAuley, Polymers Exhibiting Lower Critical Solution Temperatures as a Route to Thermoreversible Gelators for Healthcare, Adv. Funct. Mater. 2008123 (2020). doi:10.1002/adfm.202008123.

[74] E.Y. Kim, Z.G. Gao, J.S. Park, H. Li, K. Han, rhEGF/HP-β-CD complex in poloxamer gel for ophthalmic delivery, Int. J. Pharm. 233 (2002) 159–167. doi:10.1016/S0378-5173(01)00933-4.

[75] D.S. Jones, A.D. Woolfson, A.F. Brown, Textural, viscoelastic and mucoadhesive properties of pharmaceutical gels composed of cellulose polymers, Int. J. Pharm. 151 (1997) 223–233. doi:10.1016/S0378-5173(97)04904-1.

[76] J. Bassi da Silva, S.B. de S. Ferreira, O. de Freitas, M.L. Bruschi, A critical review about

methodologies for the analysis of mucoadhesive properties of drug delivery systems, Drug Dev. Ind. Pharm. 9045 (2017) 1–67. doi:10.1080/03639045.2017.1294600.

[77] I.A. Sogias, A.C. Williams, V. V. Khutoryanskiy, Chitosan-based mucoadhesive tablets for oral delivery of ibuprofen, Int. J. Pharm. 436 (2012) 602–610. doi:10.1016/j.ijpharm.2012.07.007.

[78] M.T. Cook, S.L. Smith, V. Khutoryanskiy, Novel glycopolymer hydrogels as mucosa-mimetic materials to reduce animal testing, Chem. Commun. 51 (2015) 14447–14450. doi:10.1039/C5CC02428E.

[79] N. Üstündağ Okur, N. Hökenek, M.E. Okur, Ş. Ayla, A. Yoltaş, P.I. Siafaka, E. Cevher, An alternative approach to wound healing field; new composite films from natural polymers for mupirocin dermal delivery, Saudi Pharm. J. 27 (2019) 738–752. doi:10.1016/j.jsps.2019.04.010.

[80] M.T. Cook, V. V. Khutoryanskiy, Mucoadhesion and mucosa-mimetic materials—A mini-review, Int. J. Pharm. 495 (2015) 991–998. doi:10.1016/j.ijpharm.2015.09.064.

[81] F.C. Carvalho, G. Calixto, I.N. Hatakeyama, G.M. Luz, M.P.D. Gremião, M. Chorilli, Rheological, mechanical, and bioadhesive behavior of hydrogels to optimize skin delivery systems., Drug Dev. Ind. Pharm. 39 (2013) 1750–7. doi:10.3109/03639045.2012.734510.

[82] F.J.O. Varum, F. Veiga, J.S. Sousa, A.W. Basit, Mucoadhesive platforms for targeted delivery to the colon, Int. J. Pharm. 420 (2011) 11–19. doi:10.1016/j.ijpharm.2011.08.006.

[83] J. Bassi da Silva, S.B. de S. Ferreira, A.V. Reis, M.T. Cook, M.L. Bruschi, Assessing mucoadhesion in polymer gels: The effect of method type and instrument variables, Polymers (Basel). 10 (2018) 1–19. doi:10.3390/polym10030254.

[84] C.A. Robertson, D.H. Evans, H. Abrahamse, Photodynamic therapy (PDT): A short review on cellular mechanisms and cancer research applications for PDT, J. Photochem. Photobiol. B Biol. 96 (2009) 1–8. doi:10.1016/j.jphotobiol.2009.04.001.

[85] R.D. Snook, R.D. Lowe, M.L. Baesso, A. Science, Photothermal spectrometry for membrane and interfacial region studies †, 123 (1998) 587–593.

[86] R.W. Redmond, J.N. Gamlin, A compilation of singlet oxygen yields from biologically relevant molecules, Photochem. Photobiol. 70 (1999) 391–475. doi:10.1111/j.1751-1097.1999.tb08240.x.

[87] A. Song, J. Zhang, M. Zhang, T. Shen, J. Tang, Spectral properties and structure of fluorescein and its alkyl derivatives in micelles, Colloids Surfaces A Physicochem. Eng. Asp. (2000). doi:10.1016/S0927-7757(99)00313-1.

[88] J.L. da S. Gonçalves, C. Bernal, H. Imasato, J.R. Perussi, Hypericin cytotoxicity in tumor and non-tumor cell lines: A chemometric study, Photodiagnosis Photodyn. Ther.

20 (2017) 86–90. doi:10.1016/j.pdpdt.2017.08.005.

[89] G. Grassi, A. Crevatin, R. Farra, G. Guarnieri, A. Pascotto, B. Rehimers, R. Lapasin, M. Grassi, Rheological properties of aqueous Pluronic-alginate systems containing liposomes, J. Colloid Interface Sci. (2006). doi:10.1016/j.jcis.2006.04.068.

[90] R. Bhardwaj, J. Blanchard, Controlled-release delivery system for the α-MSH analog Melanotan-I using poloxamer 407, J. Pharm. Sci. (1996). doi:10.1021/js960097g.

[91] V.R. Batistela, D.S. Pellosi, F.D. De Souza, W.F. Da Costa, S.M. De Oliveira Santin, V.R. De Souza, W. Caetano, H.P.M. De Oliveira, I.S. Scarminio, N. Hioka, PKa determinations of xanthene derivates in aqueous solutions by multivariate analysis applied to UV-Vis spectrophotometric data, Spectrochim. Acta - Part A Mol. Biomol. Spectrosc. 79 (2011) 889–897. doi:10.1016/j.saa.2011.03.027.

[92] D.S. Pellosi, B.M. Estevão, J. Semensato, D. Severino, M.S. Baptista, M.J. Politi, N. Hioka, W. Caetano, Photophysical properties and interactions of xanthene dyes in aqueous micelles, J. Photochem. Photobiol. A Chem. 247 (2012) 8–15. doi:10.1016/j.jphotochem.2012.07.009.

[93] S. Hamri, T. Bouchaour, U. Maschke, Erythrosine/triethanolamine system to elaborate crosslinked poly(2-hydroxyethylmethacrylate): UV-photopolymerization and swelling studies, Macromol. Symp. 336 (2014) 75–81. doi:10.1002/masy.201300018.

[94] J.P. Gonçalves, C.C. de Oliveira, E. da Silva Trindade, I.C. Riegel-Vidotti, M. Vidotti, F.F. Simas, In vitro biocompatibility screening of a colloidal gum Arabic-polyaniline conducting nanocomposite, Int. J. Biol. Macromol. 173 (2021) 109–117. doi:10.1016/j.ijbiomac.2021.01.101.

[95] International Organization for Standardization, Tests for in vitro cytotoxicity, Biological Evaluation and Medical Devices, 2009. http://nhiso.com/wp-content/uploads/2018/05/ISO- 10993-5-2009.pdf.

[96] M. Redhead, G. Mantovani, S. Nawaz, P. Carbone, D.C. Gorecki, C. Alexander, C. Bosquillon, Relationship between the affinity of PEO-PPO-PEO block copolymers for biological membranes and their cellular effects, Pharm. Res. 29 (2012) 1908–1918. doi:10.1007/s11095-012-0716-6.